

SPECTRAL STUDIES OF PYRENE CARBOXYLIC ACIDS

by

Jeannie Haller

• • • • •

Submitted in partial fulfillment
of the requirements for
Honors in the Department of Chemistry

UNION COLLEGE

June, 1987

JNS
1987

ABSTRACT

HALLER, JEANNIE Spectral Studies of Pyrene Carboxylic Acids. Department of Chemistry, March 1987.

The pK_a and pK_a^* of 1-pyrenecarboxylic acid (PCA) in a 50% ethanol/water solvent were experimentally determined to be 4.3 and 5.2, respectively. The pK_a of pyrene acrylic acid (PAA) in the same solvent was experimentally determined to be 4.6. An excited state equilibrium was not reached at the buffer concentrations used for the pK_a^* analysis; therefore, a valid value for the pK_a^* can not be reported at this time, but taking both the experimental results and the calculated pK_a^* 's into account, it appears that the pK_a^* of PAA is in the range $6.6 < pK_a^* < 7.4$.

The fluorescence of PCA, PAA, and 1-anthracic acid (1-AA) were studied as a function of solvent. The fluorescence of PCA was solvent independent - small spectral shifts as well as the retention of structure were observed in solvents of varying polarity. The fluorescence of 1-AA and PAA exhibited a solvent dependence.

The results of both the pK_a analysis and the fluorescence studies indicate that the S_0 and the S_1 states of PCA have a similar geometry, but that the geometry of the S_0 and the S_1 states of PAA differ. The change in geometry may be the rotation of the carboxyl group from its nearly perpendicular position with the ring in the S_0 state to a more coplanar position with the ring in the S_1 state.

The effects of hydrogen bonding in hexafluoroisopropanol on the spectral properties of PAA were studied, and the results of the studies indicate that PAA forms a hydrogen-bonded complex with hexafluoroisopropanol in both the ground and the excited states.

ACKNOWLEDGEMENTS

I would like to thank Dr. Thomas C. Werner for his guidance and support throughout this research, and for devoting additional time during the summer to this work.

I would also like to thank the organizers of the 1986 Summer Internship Program at Union College for providing me with the opportunity to continue the research on this project throughout the summer.

TABLE OF CONTENTS

	Page
Abstract	ii
Acknowledgements	iii
Index of Figures	v
Index of Tables	vii
Introduction	1
Experimental:	9
Chemicals	9
Instrumental	9
Procedure	12
Results	32
Discussion	99
References	105

INDEX OF FIGURES

Number	Title	Page
1	Jablonski Diagram	2
2	Illustration of the Frank Condon Principle	5
3	Structures of PCA, 1-AA, PAA, Hexafluoroisopropanol and Trifluoroethanol	10
4	Chromatogram of Anthracene-1-carboxylic Acid and Anthracene-2-carboxylic Acid	13
5	Chromatogram of PCA	15
6	Chromatogram of PAA Before Purification	17
7	Chromatogram of PAA After Recrystallization	20
8	Excitation Spectra of the Acidic and Basic Forms of PCA	23
9	Emission Spectra of the Acidic and Basic Forms of PCA	25
10	Emission Spectra of the Acidic and Basic Forms of PAA	29
11	Absorption of PCA as a Function of pH	34
12	Overlap of Emission and Excitation Spectra of PCA	38
13	Absorption Spectra of PCA in Dioxane, Ethanol and Ethyl Acetate	41
14	Absorption Spectra of PCA in Trifluoroethanol and Hexafluoroisopropanol	43
15	Absorption Spectra of 1-AA in Dioxane, Ethanol, Ethyl Acetate and Trifluoroethanol	45
16	Absorption Spectra of 1-AA in Cyclohexane and Hexafluoroisopropanol	47
17	Absorption Spectra of PAA in Dioxane, Ethanol, and Ethyl Acetate	49

18	Absorption Spectra of PAA in Hexafluoroisopropanol and Trifluoroethanol	51
19	Absorption Spectrum of PAA in Cyclohexane	53
20	Emission Spectrum of PCA in Dioxane	56
21	Emission Spectrum of PCA in Ethanol	58
22	Emission Spectrum of PCA in Ethyl Acetate	60
23	Emission Spectrum of PCA in Trifluoroethanol	62
24	Emission Spectra of PCA in Hexafluoroisopropanol and Cyclohexane	64
25	Emission Spectrum of 1-AA in Dioxane	66
26	Emission Spectrum of 1-AA in Ethanol	68
27	Emission Spectrum of 1-AA in Ethyl Acetate	70
28	Emission Spectrum of 1-AA in Trifluoroethanol	72
29	Emission Spectra of 1-AA in Hexafluoroisopropanol and Cyclohexane	74
30	Emission Spectrum of PAA in Dioxane	77
31	Emission Spectrum of PAA in Ethanol	79
32	Emission Spectrum of PAA in Ethyl Acetate	81
33	Emission Spectrum of PAA in Trifluoroethanol	83
34	Emission Spectrum of PAA in Hexafluoroisopropanol and Cyclohexane	85
35	PAA Absorption in Cyclohexane before and after the addition of Hexafluoroisopropanol	87
36	PAA Emission in Cyclohexane before and after the addition of Hexafluoroisopropanol	89
37	Lippert Plot for PCA	93

INDEX OF TABLES

Number	Title	Page
1	Experimentally Determined pK_a 's and pK_a^* 's	33
2	Förster Cycle Calculation of the pK_a^* of PCA	37
3	Förster Cycle Calculation of the pK_a^* of PAA	37
4	Spectral Shifts Relative to Cyclohexane	91
5	Data for Determination of s, a, and b for 1-AA from the Kamlet, Abboud, and Taft Parameterization Method	96
6	Calculation of s, a, and b for 1-AA	96
7	Data for Determination of s and a for PAA from the Kamlet, Abboud, and Taft Parameterization Method	97
8	Calculation of s and a for PAA	97
9	Results of Molecular Orbital Calculations	98

INTRODUCTION

Information about an organic molecule's structure can be obtained by studying the energy and shape of the molecule's fluorescence spectrum in various solvents.

In order to understand fluorescence, a knowledge of some basic concepts relating to molecular energy levels is required. A molecule possesses four types of energy - electronic, vibrational, rotational, and translational. In dealing with fluorescence only two types of energy levels need to be considered - electronic and vibrational - and these are depicted in the Jablonski diagram (Figure 1) (1).

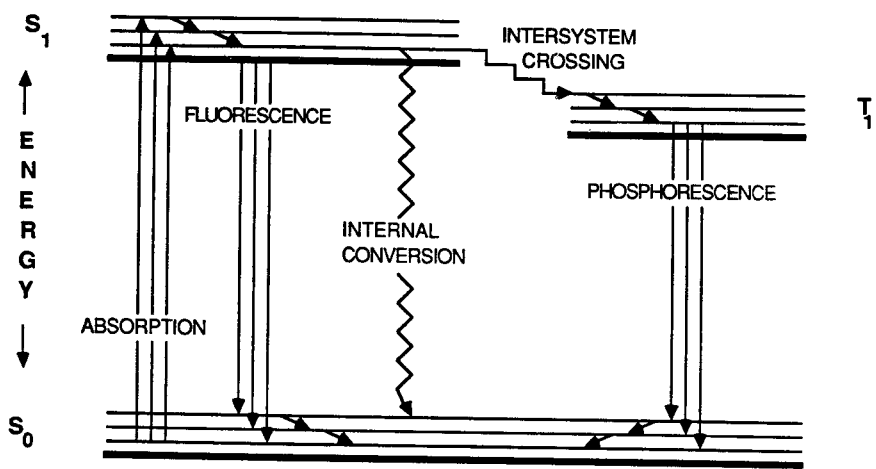
The electronic energy levels depicted are referred to as the ground state, S_0 , the first and second singlet states, S_1 and S_2 , respectively, and the first triplet state, T_1 . In the singlet states the spins of the electrons are paired, but in the triplet state the spins are parallel. Each of these electronic levels has vibrational levels associated with it.

A transition between energy levels requires a quantized amount of energy, $E=h\nu$, where h is Planck's constant and ν is the frequency of light absorbed or emitted. According to the Boltzman Distribution Law, most molecules are present in the lowest vibrational level of the ground state (1); therefore, the absorption of light results in a transition from the lowest vibrational level of the ground state to any of the vibrational levels of an excited state. This absorption process requires on the order of 10^{-14} to 10^{-15} sec (2).

Once a molecule has been excited to a higher energy level there are four primary ways it can lose its excess energy. Internal conversion is a radiationless process in which the molecule passes from one electronic state to another with no change in the

FIGURE 1

Jablonski Diagram



JABLONSKI DIAGRAM

spins of the electrons. A radiationless process in which the spin of an excited electron is reversed as it changes electronic states is called intersystem crossing (ISC). If ISC occurs, the molecule can lose the rest of its excess energy through a radiative process termed phosphorescence. The fourth means by which excess energy can be lost is fluorescence. Simply stated, fluorescence involves a radiative transition from an excited singlet state to any of the vibrational levels of S_0 , but there is actually a more complicated process involved.

Upon the absorption of light, electronic excitation occurs within approximately 10^{-14} to 10^{-15} sec (2). The Frank-Condon (FC) principle states that nuclear motion (10^{-13} to 10^{-11} sec) is much slower than electronic motion (3); therefore, immediately after excitation an excited molecule has its ground state geometry and solvent cage - the molecule is in the Frank-Condon excited state (FCES) (Figure 2) (3). Vibrational relaxation occurs almost immediately after electronic excitation, so within 10^{-13} to 10^{-14} sec molecules can be found in the lowest vibrational level of S_1 , where they remain for 10^{-9} to 10^{-7} sec before emitting (3). Because nuclear motion requires only 10^{-13} to 10^{-11} sec, there is ample time for molecular geometry changes and solvent relaxation which make the molecule more compatible with its new electron distribution to occur before emission. These changes stabilize the molecule, and when emission occurs it is from the equilibrium excited state (EQES) to the Frank-Condon ground state (FCGS). The geometry and solvent cage of the molecule in the FCGS are the same as in the EQES. Geometry changes and solvent relaxation follow emission and the molecule reaches the equilibrium ground state (EQGS).

The illustration of the Frank Condon principle in Figure 2 is very helpful in interpreting fluorescence spectra. It is evident that a molecule emits radiation from a lower energy level (EQES) than the molecule was promoted to upon absorption (FCES). This accounts for the fact that a molecule's 0-0 fluorescence band is at longer wavelengths than its 0-0 absorption band. This difference is known as the Stokes

FIGURE 2

Frank Condon Energy Diagram

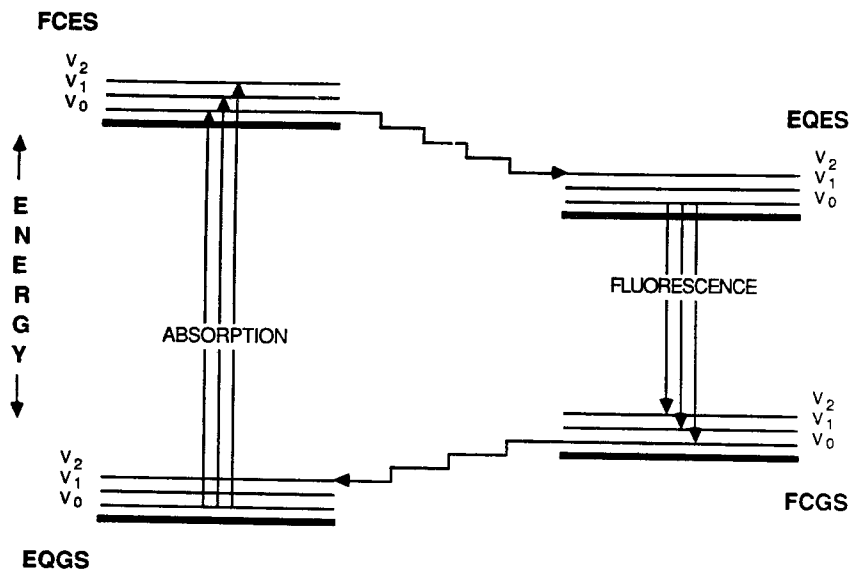


ILLUSTRATION OF THE
FRANK CONDON PRINCIPLE

shift and it is generally reported in wavenumbers.

The relationship between a molecule's geometry and its absorption and fluorescence spectra can also be accounted for by Figure 2. Some molecules, such as anthracene, have a very small Stokes shift (3). This can be attributed to the fact that its ground state geometry and its excited state geometry must be similar due to the small energy difference between the FCES and the EQES. Anthracene also has a fluorescence spectrum which is highly structured and which is the mirror image of its absorption spectrum. The fine structure implies that there are a limited number of vibrational isomers, and the mirror image relationship is indicative of similar spacing between vibrational levels of the Frank-Condon and equilibrium states.

In contrast to the fluorescence spectrum of anthracene, the spectrum of 9-anthroic acid in acidic ethanol has a large Stokes shift and it is much more diffuse (less structured) (4). A large Stokes shift is representative of differing ground and excited state geometries, and the diffuseness of the spectrum can be attributed to the overlap of vibrational bands due to emission from a large number of vibrational isomers.

The purpose of this study was to learn more about the spectral properties of 1-pyrenecarboxylic acid (PCA) and 3-(1-pyrene)propenoic acid (pyrene acrylic acid, PAA), and to use this information to determine the structure of the molecules' ground and excited states. A molecule with similar structure, 1-anthroic acid (1-AA), has been studied extensively, and it is known to have a solvent dependent fluorescence (5). A series of experiments similar to those made upon 1-AA were made in order to compare the properties of the pyrene carboxylic acids to those of 1-AA, and to relate those properties to the molecules' structures.

The study focuses on three methods which can be employed to relate spectral properties to structure. One method is a qualitative evaluation of a molecule's absorption and fluorescence spectra as explained previously.

The second method employed was used because the molecules under study were

acids. Upon excitation the electronic charge in a molecule is altered. The state formed upon excitation is called an intramolecular charge-transfer (CT) excited singlet state (6). In acids the carboxyl group is an electron acceptor; the low lying vacant π orbitals can accept electrons from the aromatic ring. The increased electron density on the functional group as a result of more extensive conjugation with the ring in the excited state makes the excited state more basic than the ground state. A comparison of the acid strength of the ground and excited state by the determination of the pK_a and the excited state pK_a (pK_a^*), respectively, provides a measure of the charge transfer which occurs. The various methods used to calculate the pK_a and pK_a^* will be enumerated upon in the later sections.

In addition to the change in pK_a which results because of the CT state, a shift in the fluorescence spectrum is generally observed. Because the carboxyl group possesses more negative character in the excited state than in the ground state due to electron density buildup, the excited state is destabilized to a greater extent upon dissociation. The greater degree of destabilization causes the FCES and the EQES to be at higher energy levels for the unprotonated form of the acid than the protonated form; therefore, the unprotonated form fluoresces at shorter wavelengths. By varying the pH of the solution, the shift of the spectrum may be observed.

The third method of analysis attempted to make a more quantitative analysis of certain molecular properties. Linear solvation energy relationships were used to determine the susceptibility of fluorescence to hydrogen-bond acceptance, hydrogen-bond donation, and polarization for PCA, 1-AA, and PAA.

EXPERIMENTAL

CHEMICALS

Spectrophotometric grade solvents were obtained from Omnisolv (hexane, isopropanol, and dimethyl sulfoxide), Aldrich (cyclohexane, methanol, ethyl acetate, p-dioxane, trifluoroethanol, and hexafluoroisopropanol), Fisher Scientific (acetone), Burdick and Jackson (acetonitrile), and Matheson Coleman and Bell (N,N-dimethylformamide). Pure grade ethanol was obtained from U.S. Industrial Chemicals. PAA and PCA were from Molecular Probes, Inc.. 1-AA had been synthesized in earlier experiments, and it had a melting point of 244-246°C. For the buffers, the $\text{NaH}_2\text{PO}_4 \cdot \text{H}_2\text{O}$, $\text{Na}_2\text{HPO}_4 \cdot 7\text{H}_2\text{O}$, and $\text{NaC}_2\text{H}_3\text{O}_2$ were Mallinckrodt, Fischer, or Aldrich reagent grade chemicals; hydrochloric acid and acetic acid were from Fischer; and phosphoric acid was from J.T. Baker Chemical Company. The structures of PCA, 1-AA, and PAA are shown in Figure 3. Hexafluoroisopropanol and trifluoroethanol are not commonly used solvents; therefore, their structures are also shown in Figure 3.

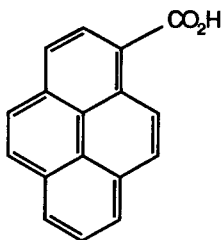
INSTRUMENTAL

Absorption measurements were made on a Perkin-Elmer Lambda 3B UV/VIS spectrophotometer or a Cary 118C spectrophotometer.

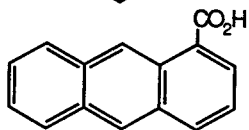
High-performance liquid chromatography was performed using a Varian Model

FIGURE 3

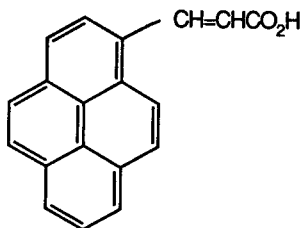
Structures of PCA, 1-AA, PAA, Hexafluoroisopropanol and Trifluoroethanol



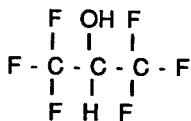
1-PYRENECARBOXYLIC ACID



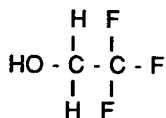
1-ANTHROIC ACID



PYRENE ACRYLIC ACID



1,1,1,3,3,3-HEXAFLUORO-2-PROPANOL



2,2,2-TRIFLUOROETHANOL

5000 liquid chromatograph with a reverse phase C₁₈ column. Water and acetonitrile were used as the mobile phases.

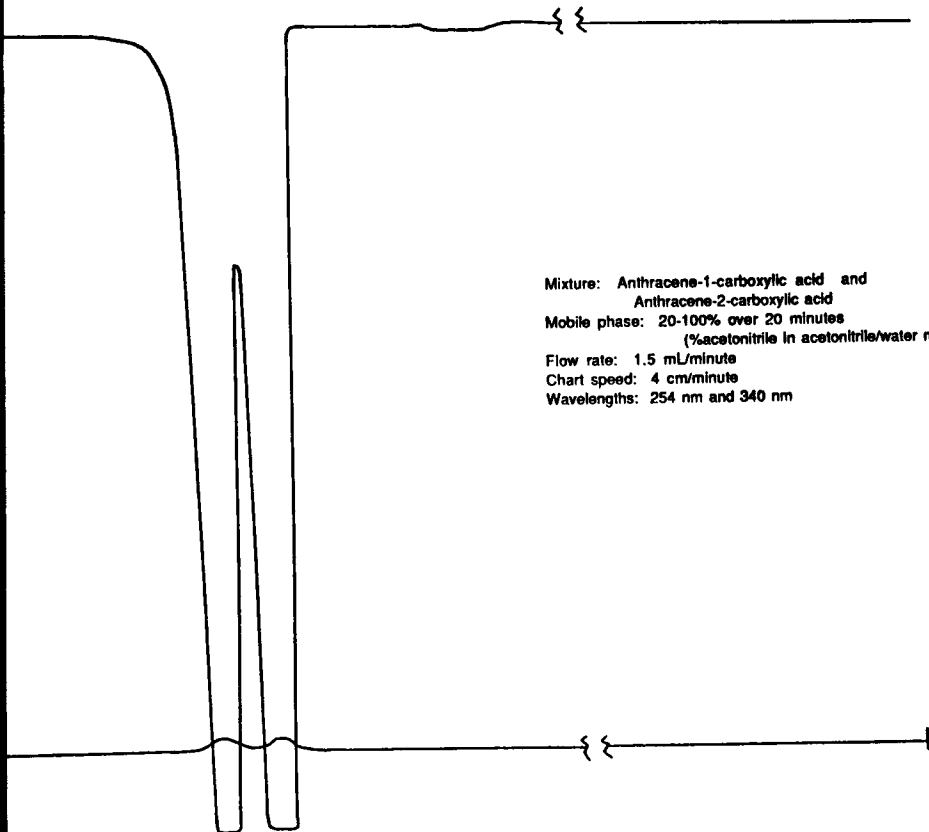
Fluorescence spectra were recorded at room temperature on a Perkin-Elmer Hitachi-MPF-2A spectrofluorometer interfaced to an Apple computer. The spectra were corrected for the response function of the instrument as described in the interface manual (7).

PROCEDURE

High-performance liquid chromatography (HPLC) was used to determine the purity of the PCA and PAA samples. In order to determine the validity of our HPLC program as a separation technique, it was tested on a known mixture. A solution containing anthracene-1-carboxylic acid and anthracene-2-carboxylic acid was made and analyzed by HPLC. This mixture was chosen because if there were impurities in the PCA and PAA samples, it was highly probable that they were other pyrene carboxylic acids. Two peaks were clearly distinguishable on the chromatogram (Figure 4); therefore, the separation method was assumed to be valid. Analysis of the PCA using the same HPLC conditions indicated that it was pure - only one peak was observed on the chromatogram (Figure 5). The PAA samples were not pure - two peaks were clearly distinguishable on the chromatogram of each sample (Figure 6A), thus indicating the elution of two components. A variation was made in the method in order to reduce the time required to run a chromatogram. The mobile phase was started with a higher percentage of acetonitrile and the time required to take the chromatogram was reduced. As a result of these changes the percentage of acetonitrile in the mobile phase increased at a rate of six per cent per minute rather than four per cent per minute, but the validity as a separation technique was preserved as shown in Figure

FIGURE 4

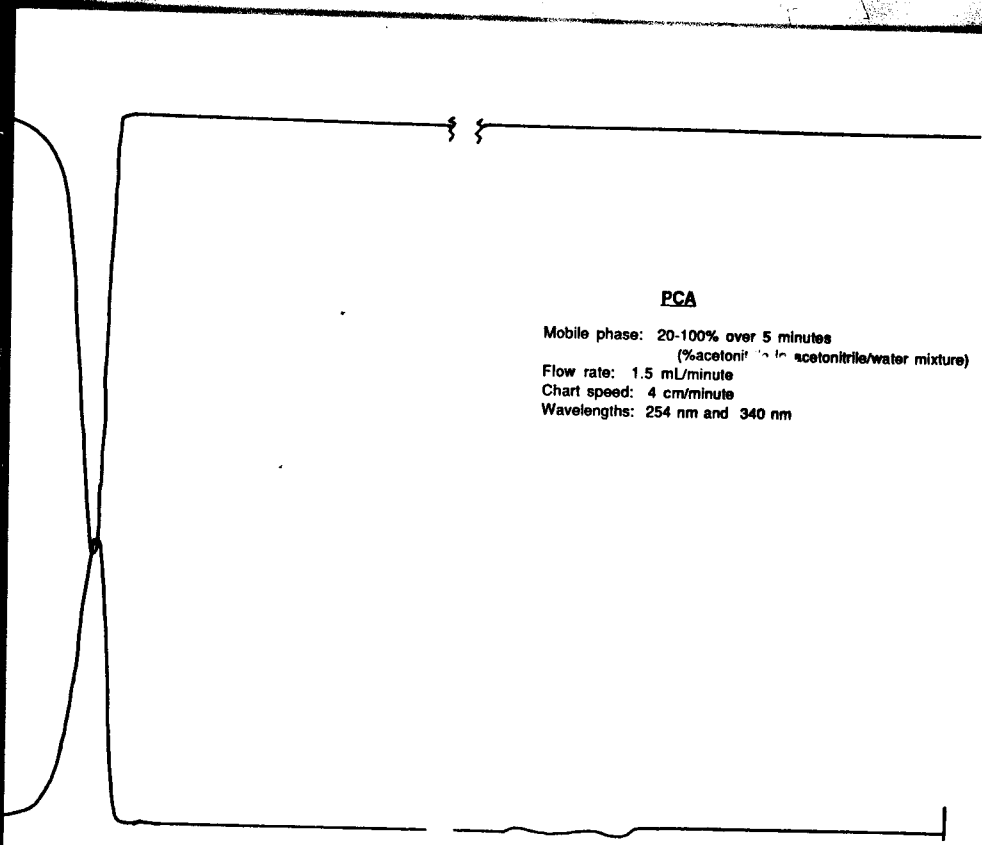
**Chromatogram of Anthracene-1-carboxylic Acid
and Anthracene-2-carboxylic Acid**



Mixture: Anthracene-1-carboxylic acid and
Anthracene-2-carboxylic acid
Mobile phase: 20-100% over 20 minutes
(%acetonitrile in acetonitrile/water mixture)
Flow rate: 1.5 mL/minute
Chart speed: 4 cm/minute
Wavelengths: 254 nm and 340 nm

FIGURE 5

Chromatogram of PCA

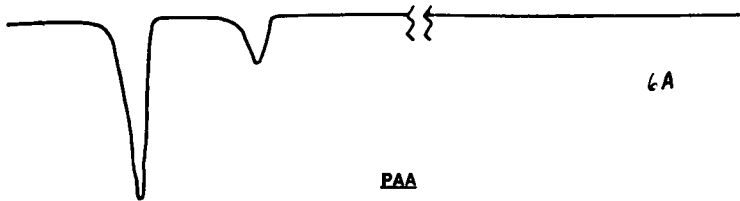


PCA

Mobile phase: 20-100% over 5 minutes
(%acetonitrile to acetonitrile/water mixture)
Flow rate: 1.5 mL/minute
Chart speed: 4 cm/minute
Wavelengths: 254 nm and 340 nm

FIGURE 6

Chromatogram of PAA Before Purification



6A

PAA

Mobile phase: 20-100% over 20 minutes
(%acetonitrile in acetonitrile/water mixture)
Flow rate: 1.5 mL/minute
Chart speed: 4 cm/minute
Wavelengths: 254 nm and 340 nm



PAA

Mobile phase: 70-100% over 5 minutes
(%acetonitrile in acetonitrile/water mixture)
Flow rate: 1.5 mL/minute
Chart speed: 4 cm/minute
Wavelength: 340 nm

6B



18

6B, which is a chromatogram obtained from the analysis of the same sample as the chromatogram in 6A, but which was obtained using the new method.

A separation of the two components found for PAA was attempted in order to obtain a reasonably pure quantity of PAA. No change in the PAA chromatogram was observed after the sample was extracted with a base and acidified; thereby, indicating that the impurity was probably an acid. At this point the method of preparation of the PAA was checked with the source company, and it was determined that the sample was probably a mixture of the *cis* and *trans* isomers of PAA. Separation by thin-layer chromatography and column chromatography was attempted, but the retention times of both components were so similar that neither method proved useful. Recrystallization with methanol proved to be the most efficient method of separation. Prior to recrystallization the unwanted component comprised thirteen per cent or more of the sample by HPLC analysis. After recrystallization the percentage of the unwanted component was estimated (by HPLC, Figure 7) to be approximately three per cent.

The pK_a of PCA was determined in two mixed solvents, 30% ethanol/water and 50% ethanol/water. Eleven solutions of varying pH were made for each mixed solvent, and the absorbance of each solution was measured at 358.8nm for the 50% ethanol solutions and 360.0nm for the 30% ethanol solutions. At these wavelengths the absorption is primarily from the acidic form of the molecule. One centimeter cells were used and each solution was run against a reference cell containing the solvent used.

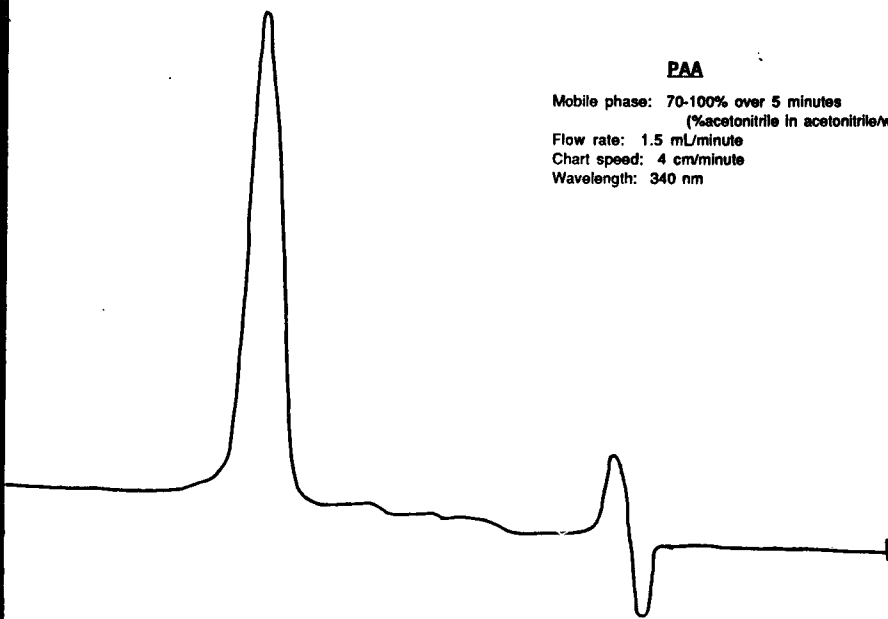
There were two reasons for using a mixed solvent rather than a purely aqueous one. PCA is not very soluble in water; therefore, the use of the ethanol/water solvent permitted the attainment of solutions with a greater concentration of PCA, which resulted in more accurate absorption measurements due to an increased absorbance. Because there was no significant difference between the results obtained in 30% ethanol and those obtained in 50% ethanol, 50% ethanol was chosen as the solvent for future work with the anticipation that PAA would be less soluble than PCA. A

FIGURE 7

Chromatogram of PAA After Recrystallization

PAA

Mobile phase: 70-100% over 5 minutes
(%acetonitrile in acetonitrile/water mixture)
Flow rate: 1.5 mL/minute
Chart speed: 4 cm/minute
Wavelength: 340 nm



second reason for using a mixed solvent was to avoid aggregation.

Pyrene-1-carboxaldehyde is known to aggregate (8), and the structures of PCA and PAA are similar to that of pyrene-1-carboxaldehyde; therefore, it was anticipated that they might also have a tendency to aggregate in aqueous solution.

For the determination of the pK_a^* of PCA, fluorescence measurements were made using excitation and emission band widths of 7 and 4nm, respectively. The solutions (and all other solutions for fluorescence work) were made having an absorption less than .05 at the wavelength of maximum absorption so that self-absorbance would not distort the spectrum. Two methods were used to determine the pK_a^* . The first method, method I, was chosen with the assumption that the pK_a^* could be obtained from a fit of the data with the Henderson-Hasselbach equation as will be explained in the results section. Solutions of varying pH were made, and the fluorescence intensity was measured as a function of pH. The solutions were excited at 385nm and the fluorescence intensity was measured at 440nm. The choice of excitation and emission wavelengths ensures that the emission of only one form of PCA, the protonated form, was monitored (Figures 8 and 9).

A second method, method II, was employed when it was determined that ΔpK_a for PCA was small. It is possible that the pK_a^* calculated using the previously stated method would appear lower than it actually is if ΔpK_a is small. This would occur if the two fluorometric curves "ran into each other". The following diagram attempts to depict this situation.



FIGURE 8

Excitation Spectra of the Acidic and Basic Forms of PCA

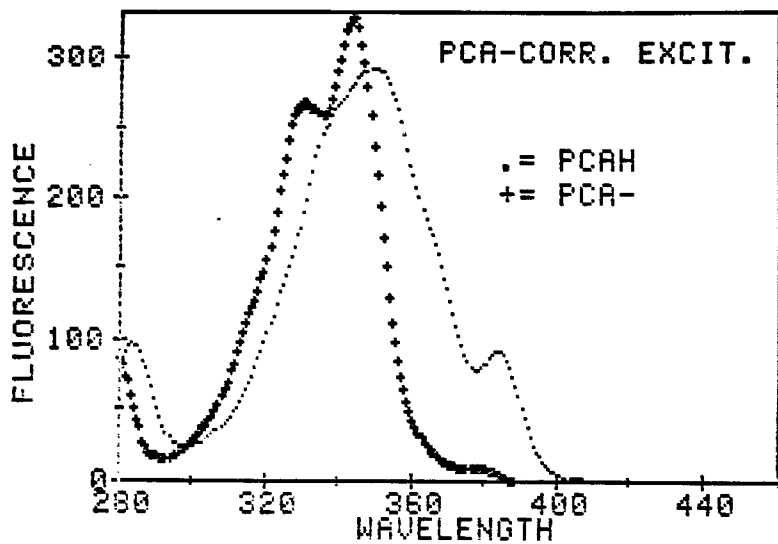
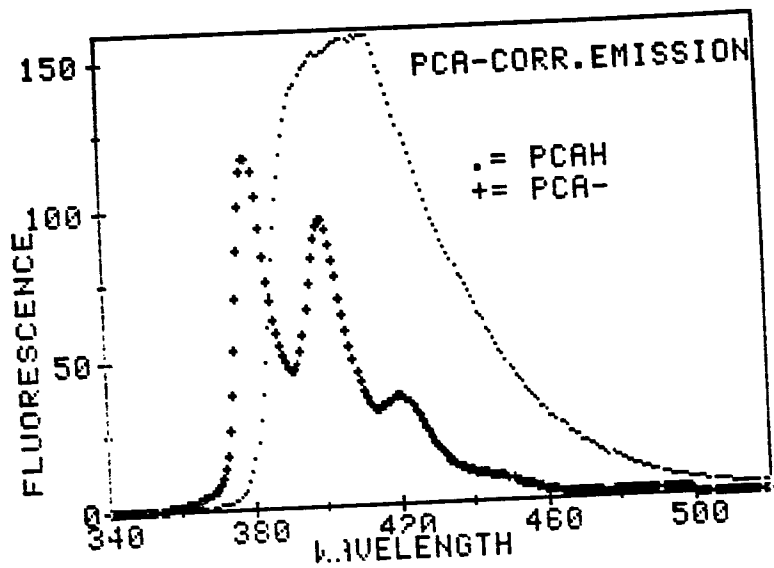


FIGURE 9

Emission Spectra of the Acidic and Basic Forms of PCA



If the curve for the ground state never leveled off, but ran into the curve for the excited state, the inflection point (X) would make the pK_a^* appear to be lower than it actually is (O). To avoid this situation, it was attempted to selectively monitor the fluorescence of the unprotonated form and to fit the data to obtain the pK_a^* . The fluorescence intensity of solutions of varying pH, all at least one pH unit greater than the value obtained for the pK_a , were measured at a given wavelength. The solutions were excited at 320nm and the fluorescence intensity was measured at 380nm. The method and the choice of emission wavelength ensures that the emission monitored was primarily from the unprotonated form of the molecule. The choice of 320nm as the excitation wavelength was not extremely important because the solutions were made at pH's in which the molecule is primarily in the unprotonated form in the ground state; therefore, at any excitation wavelength only a small percentage of the molecule excited could possibly be from the protonated form. At 380nm emission is almost entirely from the unprotonated form of the molecule (Figure 9); therefore, even if the protonated form was excited, the choice of emission wavelength ensures that the emission of primarily the unprotonated form was monitored. The intensity of the most basic solution was assigned the value of F_0 , and the intensity of the other solutions the value of F . The quantity F/F_0 was plotted as a function of pH and was fit with a third degree polynomial. The ratio F/F_0 is a ratio of the fluorescence intensity of the unprotonated form of the molecule at a specific pH to the total fluorescence intensity of the molecule. The pH at which this ratio has a value of .5 is equivalent to the pK_a^* ; therefore, the pK_a^* was calculated using the equation obtained from the polynomial fit.

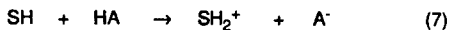
Three methods were used to determine the pK_a^* of PAA. Although changes were made in the emission band pass and the excitation and emission wavelengths, two of the methods employed were the same as those used for the determination of the pK_a^* of PCA. All measurements were made using excitation and emission band passes of 7

and 3nm, respectively.

For method I, the solutions were excited at 350nm and the fluorescence intensity was measured at 420nm. Although the choice of 420nm as the emission wavelength allowed us to measure the emission of primarily the unprotonated form(Figure 10), some emission(particularly at low pH's) is from the protonated form, because it was not possible to selectively excite the unprotonated form. For method II the solutions were excited at 380nm and the fluorescence intensity measured at 420nm. As with PCA, this method and the choice of emission wavelength ensures that the emission of primarily the unprotonated form was monitored. The third method employed, method III, was actually only a variation of method I. In method III a correction for background fluorescence from the protonated form was made. This was done because the unprotonated form could not be selectively excited. The values obtained for the pK_a^* using methods I and III were within experimental error of each other; therefore, no further distinction will be made between the two methods.

In order to determine whether the pK_a^* of both PCA and PAA were buffer dependent, it was determined at three buffer concentrations. Measurements were made in .001M and .01M phosphate buffer and .10M acetate buffer. The .10M acetate buffer was used rather than .10M phosphate buffer because the phosphate buffer did not cover the desired range due to the insolubility of Na_2HPO_4 in the 50% ethanol/water solvent at a .10M concentration.

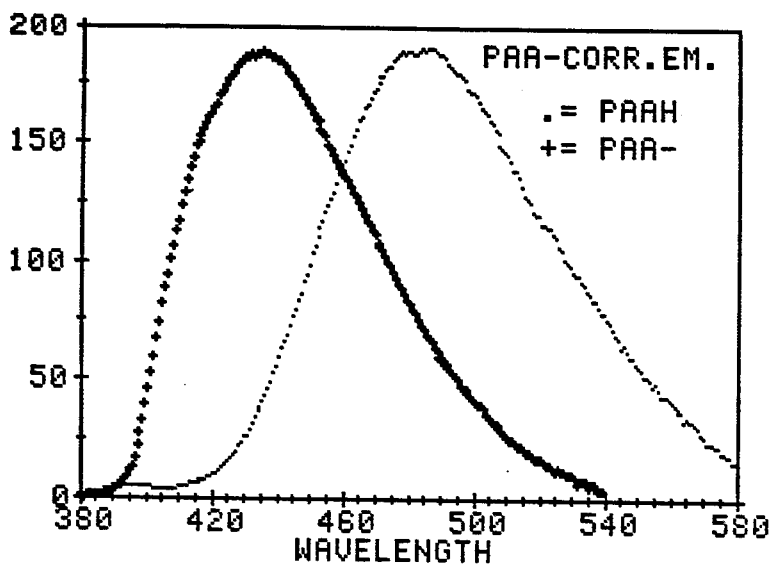
In solutions with no buffer present, the strength of as acid is determined by the equilibrium constant of the following reaction,



where HA is the acid, SH is the solvent, and A^- and SH_2^+ are the conjugate base and acid, respectively.

FIGURE 10

Emission Spectra of the Acidic and Basic Forms of PAA



In solutions containing buffer ions, the reaction in equation 7 can be accompanied by the reaction in equation 8 (6),



in which the buffer ions act as proton acceptors (D) and donors (DH⁺). Schulman's treatment of buffered systems (6) leads to the conclusion that if the buffer concentration is high enough to sustain excited-state equilibria in equation 8, the equilibrium will correspond to that obtained in a nonbuffered system such as the one represented in equation 7. The determination of a molecule's buffer dependence is indicative of the nature of the excited state as will be enumerated upon in the discussion.

Emission spectra of PCA, 1-AA, and PAA in various solvents were recorded. Excitation and emission band passes of 7 and 3nm, respectively, were used. The PCA solutions were excited at 330nm, the 1-AA solutions at 370nm, and the PAA solutions at 350, 360, or 370nm, depending upon which wavelength was closest to the wavelength of maximum absorption.

RESULTS

Absorption data were used to calculate the pK_a of PCA and PAA from equation 1 (9),

$$pK_a = pH - \log [(A - A_{AH}) / (A_A - A)] \quad (1)$$

where A_{AH} is the absorbance of the acid at the selected wavelength if the molecule is in the protonated form, A_A is the absorbance of the base at the selected wavelength if the molecule is in the unprotonated form, and A is the absorbance of the molecule at an intermediate pH. For each solution the pH was plotted versus the log term and the value of the y intercept of the resulting line was equal to the pK_a . The experimentally determined pK_a 's are listed in Table 1. Values of 4 and 3.1 for the pK_a of PCA in aqueous solution have been reported by Vander Donkt et al. (10) and Escabi-Perez and Fendler (11), respectively.

The observation of an isosbestic point for PCA (Figure 11) indicates that PCA probably underwent a simple acid-base reaction. An isosbestic point was not observed over the entire pH range for PAA; this indicates that the acid-base reaction may have been complicated by other phenomena.

The pK_a^* of PCA and PAA were experimentally determined from the data obtained using method I, as described in the experimental section, by fitting points to the Henderson-Hasselbach equation (6),

$$pH = pK_a^* + \log [(F_{AH} - F) / (F - F_B)] \quad (2)$$

where F_{AH} and F_B are the intensity of fluorescence of the acidic form and basic form,

TABLE 1

Experimentally Determined pK_a 's and pK_a^* 's

<u>COMPOUND</u>	<u>METHOD^a</u>	<u>BUFFER</u>	<u>pK_a</u>	<u>pK_a^*</u>
PCA	I	.001M P	-	5.2
PCA	I	.01M P	-	5.2
PCA	I	.10M A	-	5.2
PCA	I	.01M A	4.3	-
PCA	II	.01M P	-	5.1
PCA	II	.10M A	-	5.4
PAA	I	.01M A	4.6	5.7
PAA	I, II	.01M P	-	5.7
PAA	I	.10M A	-	6.7
PAA	II	.10M A	-	6.1

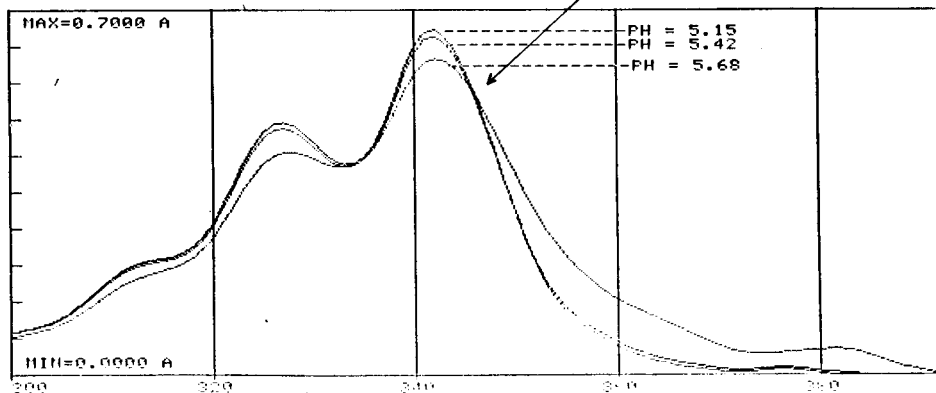
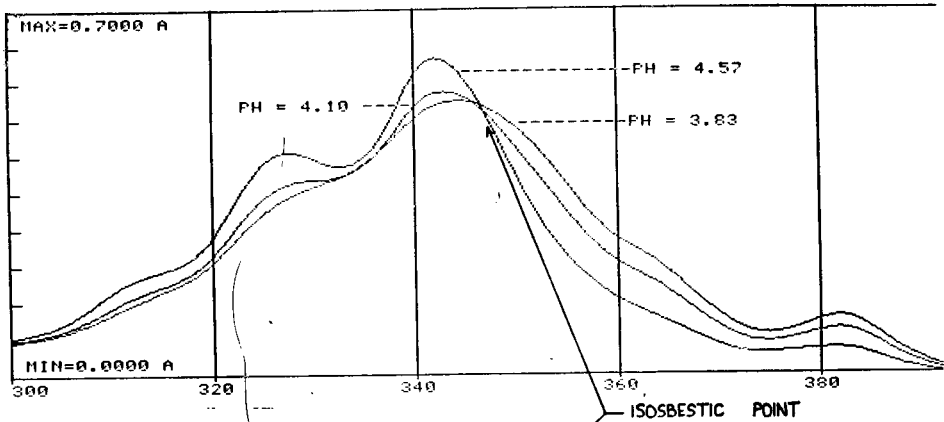
^a refers to experimental methods

I - calculated using the Henderson-Hasselbach equation
standard deviation in pK_a and $pK_a^* = \pm .1$

II - calculated from F/F_0 using polynomial fit
standard deviation in pK_a and $pK_a^* = \pm .2$

FIGURE 11

Absorption of PCA as a Function of pH



respectively, at the selected wavelength if the molecule is in the respective forms, and F is the fluorescence intensity of the molecule at an intermediate pH. The same type of data analysis was made for the pK_a^* as the pK_a , and the values obtained are listed in Table 1. The values obtained using method II are also listed in Table 1. Escabi-Perez and Fendler have reported a value of 4.2 for the pK_a^* of PCA in aqueous solution (11). Vander Donkt et al. have reported a value of 8.1 (10), but this value was obtained from the Förster cycle calculation and not experimentally.

The pK_a^* of PCA and PAA was also calculated from the Förster cycle (equation 3), and the values obtained are listed in Table 2 and Table 3, respectively. Using equation 3 (6)

$$pK_a - pK_a^* = 2.10 \cdot 10^{-3} (\bar{\nu}_A - \bar{\nu}_B) \quad (3)$$

a value for $(pK_a - pK_a^*)$ was obtained, and this value was subtracted from the pK_a determined in 50% ethanol to obtain the pK_a^* . The $(\bar{\nu}_A - \bar{\nu}_B)$ term represented different entities for different methods, but in all calculations the A and B subscripts denote the protonated and unprotonated forms of the molecule, respectively.

For the Förster cycle calculations for PCA, one method involved the use of absorption data. In that case $\bar{\nu}_A$ and $\bar{\nu}_B$ represent the wavenumbers of the 0-0 bands of absorption. Another method was based upon both absorption and fluorescence measurements. For that calculation $\bar{\nu}_A$ and $\bar{\nu}_B$ represent the wavenumber of the average of the 0-0 absorption band and the 0-0 fluorescence band. The other methods employed were based solely on fluorescence data. In one case the emission and excitation spectra for a specific form were normalized to the same intensity and overlapped (Figure 12). The point where the spectra for the acidic form overlap is $\bar{\nu}_A$ and the corresponding point for the basic form is $\bar{\nu}_B$. In the other two calculations $\bar{\nu}_A$ and $\bar{\nu}_B$ represent the wavenumbers of the 0-0 fluorescence bands and the mean frequency of fluorescence, $\bar{\nu}_m$. The mean frequency of fluorescence is a measure of

TABLE 2
Förster Cycle Calculation of the pK_a* of PCA

Method ^a	pK _a -pK _a ^{*b}	pK _a ^{*c}
0-0 Absorption Bands	-0.8	5.1
Average of Abs. and Fluor. 0-0 bands	-1.9	6.1
Fluor. Emiss. and Excit. Overlap	-2.1	6.4
Mean Frequency of Fluorescence	-2.2	6.5
0-0 Fluorescence Bands	-2.7	7.0

TABLE 3
Förster Cycle Calculation of the pK_a* of PAA

Method ^a	pK _a -pK _a ^{*b}	pK _a ^{*d}
Frequency of Max. Absorbance	-0.8	5.4
Average of Abs. and Fl. Maxima	-2.3	6.9
Average of Abs. Max. and Fl. Mean Freq.	-2.7	7.3
Mean Frequency of Fluorescence	-4.6	9.2
Frequency of Max. Fluor. Intensity	-3.8	8.4

^amethod indicates how values for ν_A and ν_B were obtained

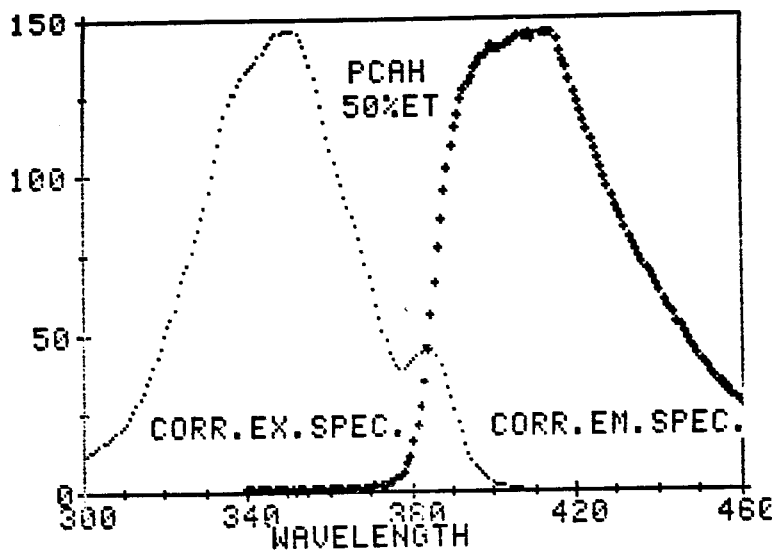
^bfrom equation 3

^cbased on pK_a=4.3 in 50% ethanol

^dbased on pK_a=4.6 in 50% ethanol

FIGURE 12

Overlap of Emission and Excitation Spectra of PCA



the average energy of S_1 as defined by equation 4 (12).

$$\int_{\bar{\nu}_i}^{\bar{\nu}_f} F(\bar{\nu})d\bar{\nu} = 2 \int_{\bar{\nu}_i}^{\bar{\nu}_m} F(\bar{\nu})d\bar{\nu} \quad (4)$$

The initial frequency is $\bar{\nu}_i$, the final frequency is $\bar{\nu}_f$, the mean frequency is $\bar{\nu}_m$, and the fluorescence intensity at a given frequency is $F(\bar{\nu})$. The mean frequency is generally used in calculations when spectra are too diffuse to determine accurately the location of the 0-0 band.

The Förster cycle calculations for PAA had to be varied slightly from those of PCA. The 0-0 band for the acidic form of the molecule was not easily distinguished and the fluorescence spectra were too diffuse to locate the 0-0 band; therefore, the frequency of the maximum absorbance or of the maximum fluorescence intensity was used in calculations rather than the 0-0 bands.

The absorption and fluorescence emission spectra of PCA, 1-AA, and PAA were recorded in solvents of varying polarity to determine the sensitivity of the molecules to solvent effects. The absorption spectra of PCA are shown in Figures 13 and 14. Although the spectra were not normalized, the similarities between the spectra in ethanol, dioxane, and ethyl acetate (Figure 13) are evident. Each has a similar structure and there is only a shift of approximately 5nm of the spectrum in the three solvents. The spectra in highly protic solvents (Figure 14) exhibit a solvent dependence; the two spectra in the highly protic solvents are shifted and they have different shapes.

The absorption spectra of 1-AA are presented in Figures 15 and 16. The spectra show that the absorption of 1-AA is solvent dependent; the shape and location of the spectrum varied, depending upon the solvent.

The absorption spectra of PAA (Figures 17-19) indicate a solvent dependence similar to that of PCA. In ethanol, dioxane, and ethyl acetate there is not a significant difference in the spectra, but in highly protic solvents the spectra are shifted and there

FIGURE 13

Absorption Spectra of PCA in Dioxane, Ethanol, and Ethyl Acetate

PCA ABSORPTION AS A FUNCTION
OF SOLVENT

$\lambda_{MAX} = 2.4500 \text{ \AA}$

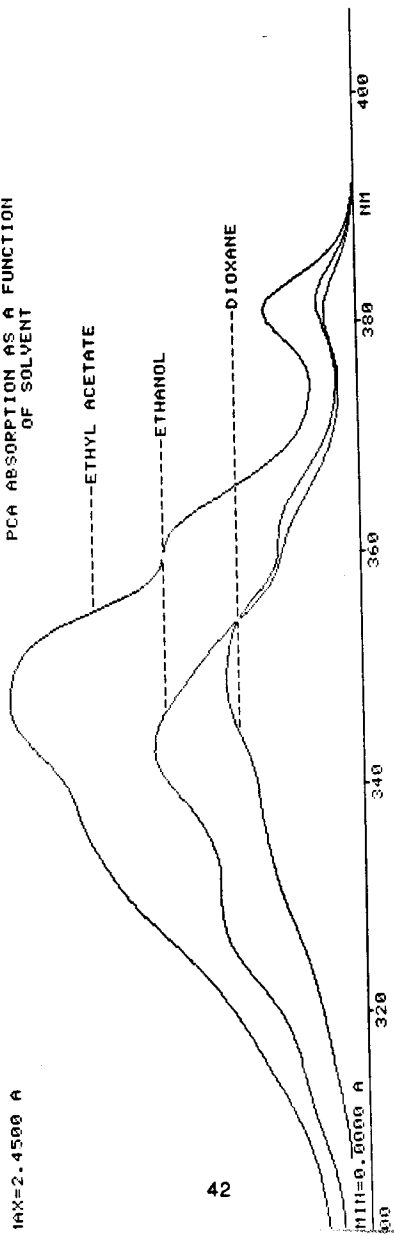


FIGURE 14

Absorption Spectra of PCA in Trifluoroethanol and Hexafluoroisopropanol

PCA ABSORPTION AS A FUNCTION OF SOLVENT

MAX=0.0600 A

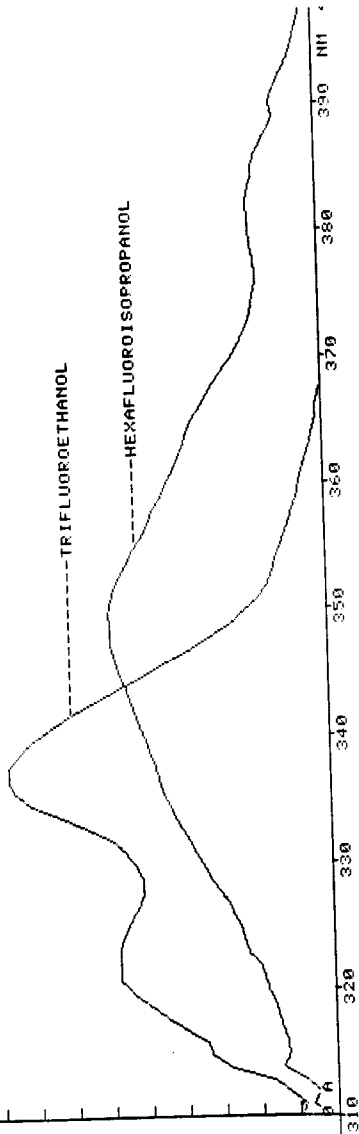


FIGURE 15

Absorption Spectra of 1-AA in Dioxane, Ethanol,
Ethyl Acetate, and Trifluoroethanol

MAX=0.6000 A

I-AA ABSORPTION AS A FUNCTION
OF SOLVENT

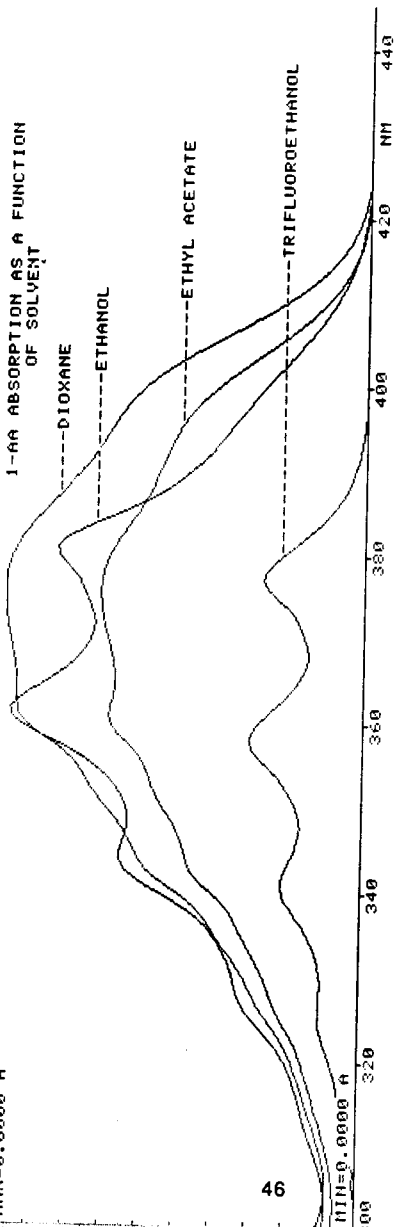


FIGURE 16

Absorption Spectra of 1-AA in Cyclohexane and Hexafluoroisopropanol

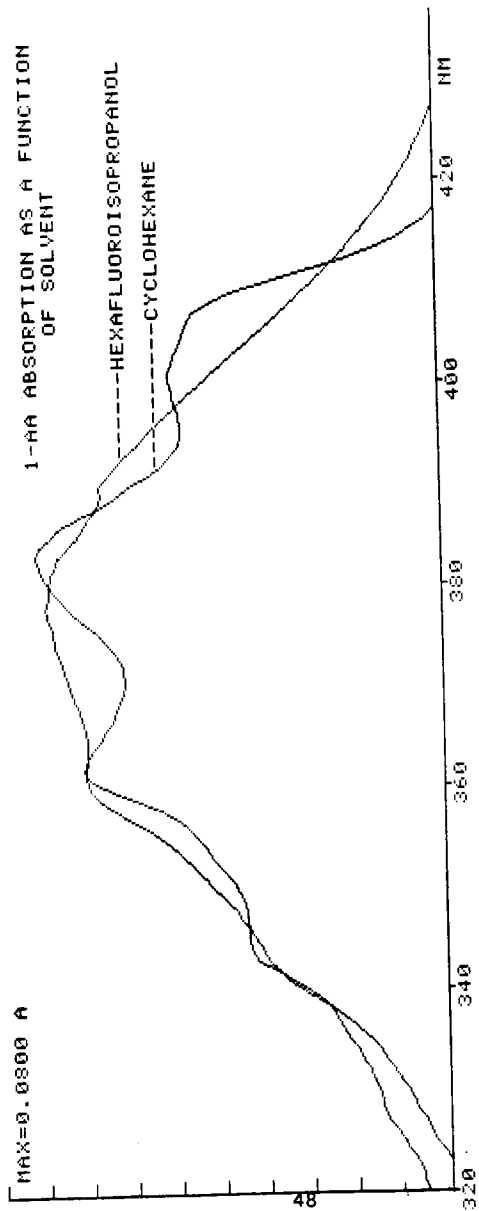


FIGURE 17

Absorption Spectra of PAA in Dioxane, Ethanol, and Ethyl Acetate

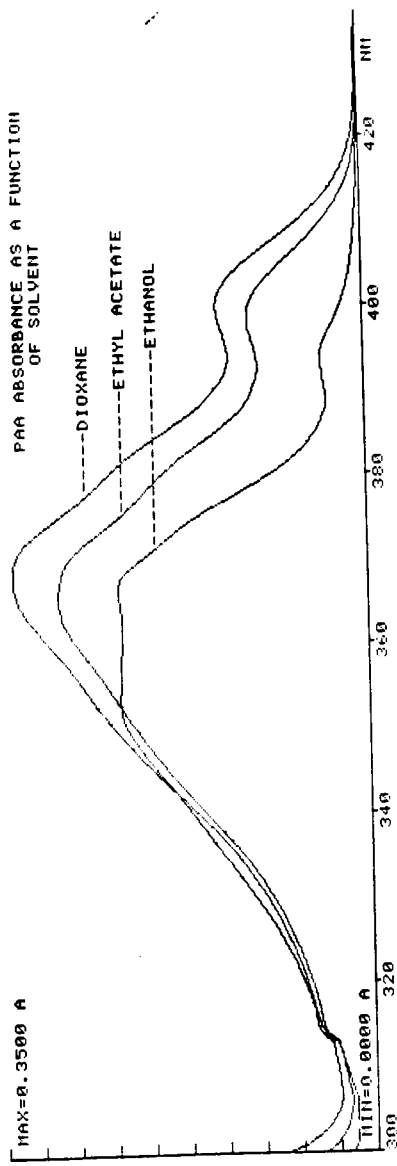


FIGURE 18

Absorption Spectra of PAA in Hexafluoroisopropanol and Trifluoroethanol

PAA ABSORBANCE AS A FUNCTION OF SOLVENT

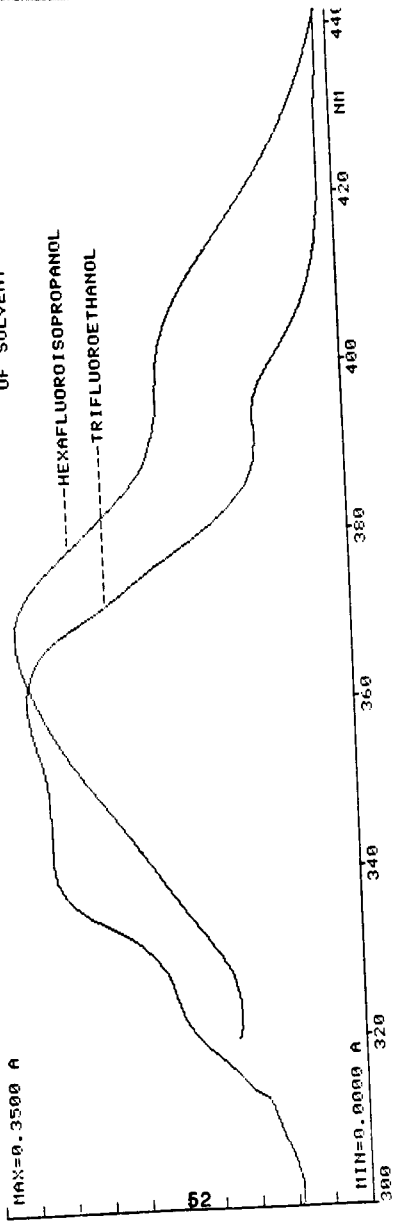
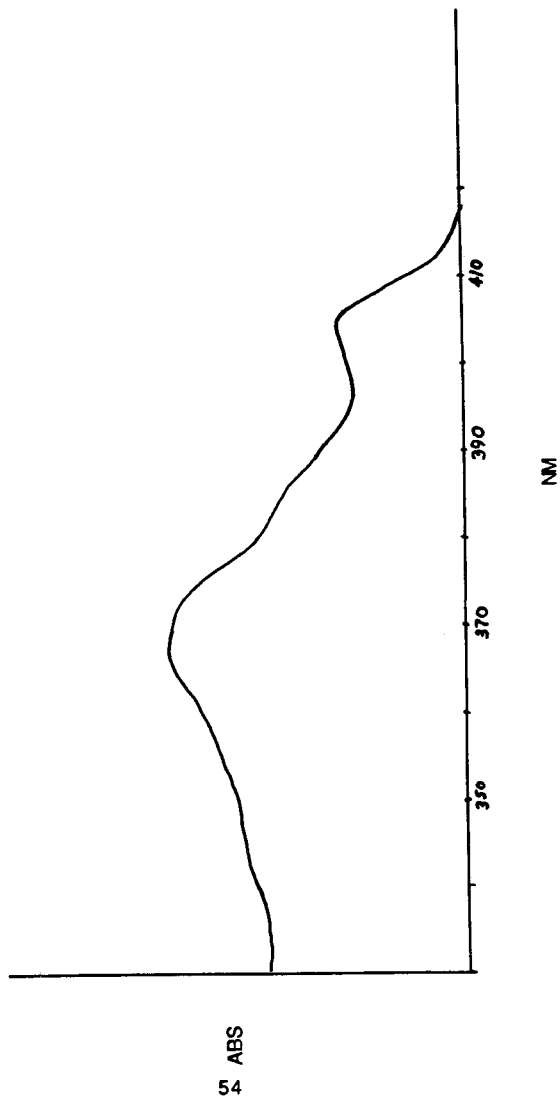


FIGURE 19

Absorption Spectrum of PAA in Cyclohexane

ABSORPTION SPECTRUM OF PAA
IN CYCLOHEXANE



is a change in shape.

The fluorescence emission spectra of PCA were recorded in twelve solvents of varying polarity. Spectra in some representative solvents are shown in Figures 20-24. It is evident that all of the spectra show a good deal of structure. The location of three vibronic bands can easily be determined for three of the solvents (cyclohexane, dioxane, and ethyl acetate); for the other three solvents (ethanol, trifluoroethanol, and hexafluoroisopropanol) two vibronic bands can easily be distinguished, and it is evident that there is a third band although the location of its maximum can not be determined accurately.

The location of the vibronic bands in these various solvents should also be noted. There is a very small shift, if any, in the location of the maximum of the 0-0 vibronic band relative to that of cyclohexane for the solvents dioxane, ethyl acetate, and ethanol. A small blue shift (shift to shorter wavelengths) of the 0-0 vibronic band occurs in hexafluoroisopropanol and trifluoroethanol. The overlap of the spectra in Figure 24 exemplify how solvent independent the fluorescence of PCA is. Cyclohexane is a nonpolar solvent which does not have the capability for hydrogen bond donation or acceptance. Hexafluoroisopropanol is a strong hydrogen bond donor, but a very weak hydrogen bond acceptor. The fact that the emission spectra of PCA are similar in these two solvents which have very different properties is indicative that its fluorescence is solvent independent.

In contrast to PCA, the fluorescence of 1-AA has a significant solvent dependence. Spectra of 1-AA taken in the solvents reported for PCA are presented in Figures 25-29. Diffuse emission spectra were obtained in all solvents but cyclohexane. The spectrum in each solvent was red-shifted relative to that observed in cyclohexane. In Figure 29 the solvent dependence in hexafluoroisopropanol relative to cyclohexane as well as the diffuseness of the spectrum in a polar solvent are easily noted. The fluorescence spectra of PAA in the chosen solvents are presented in

FIGURE 20

Emission Spectrum of PCA in Dioxane

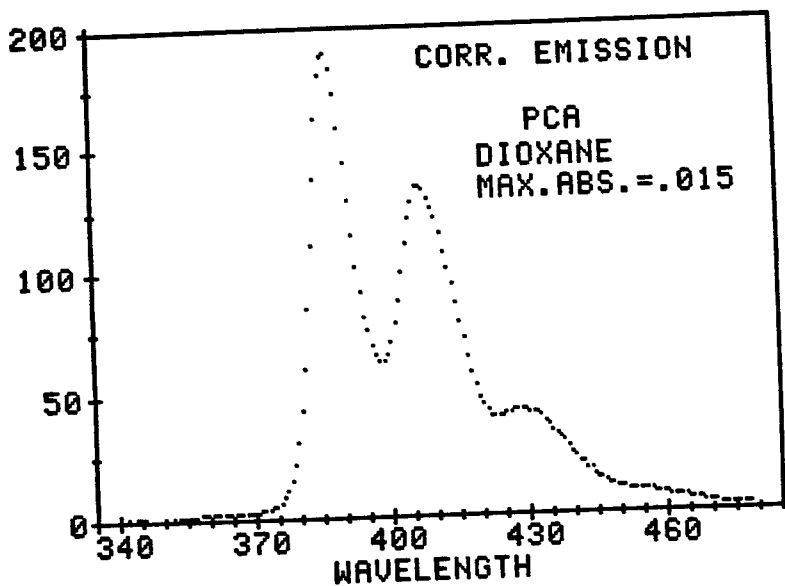


FIGURE 21

Emission Spectrum of PCA in Ethanol

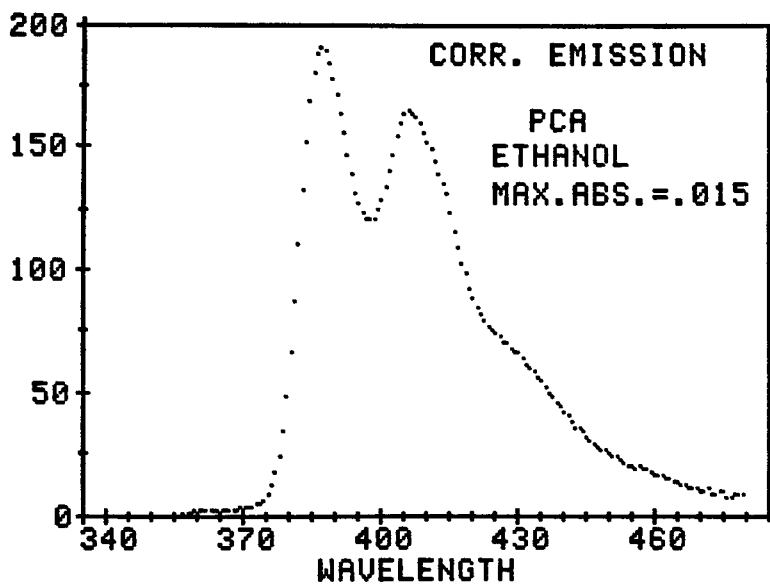


FIGURE 22

Emission Spectrum of PCA in Ethyl Acetate

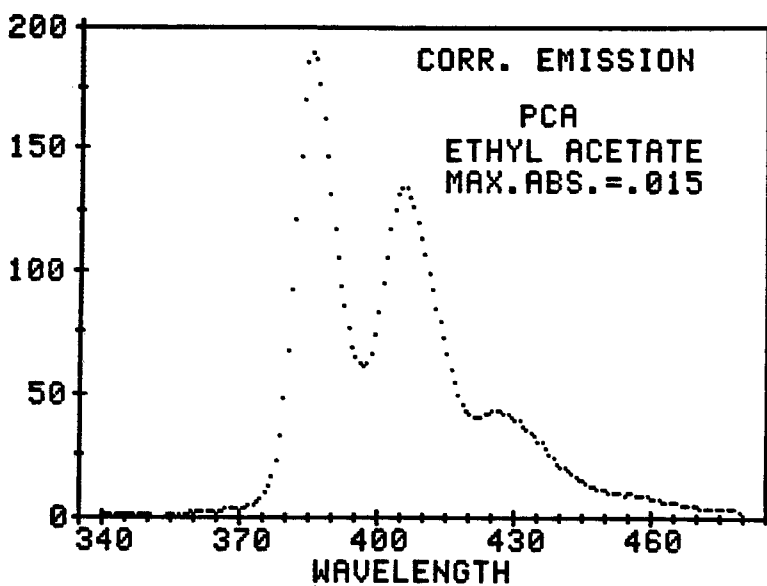


FIGURE 23

Emission Spectrum of PCA in Trifluoroethanol

UN82 HALLER, J. SPECTRAL STUDIES OF PYRENE, etc.

HI85/1987

Chemistry

HRS. 6/87

2 of 2



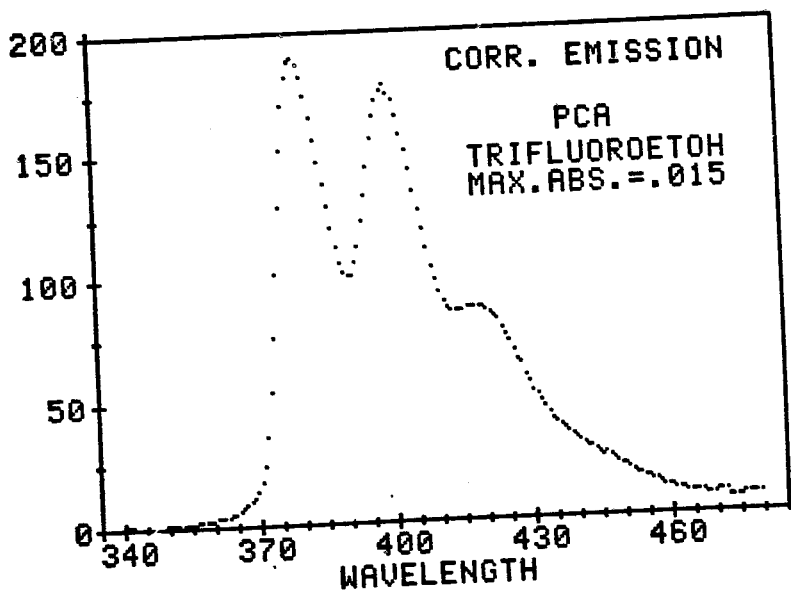


FIGURE 24

Emission Spectra of PCA in Hexafluoroisopropanol and Cyclohexane

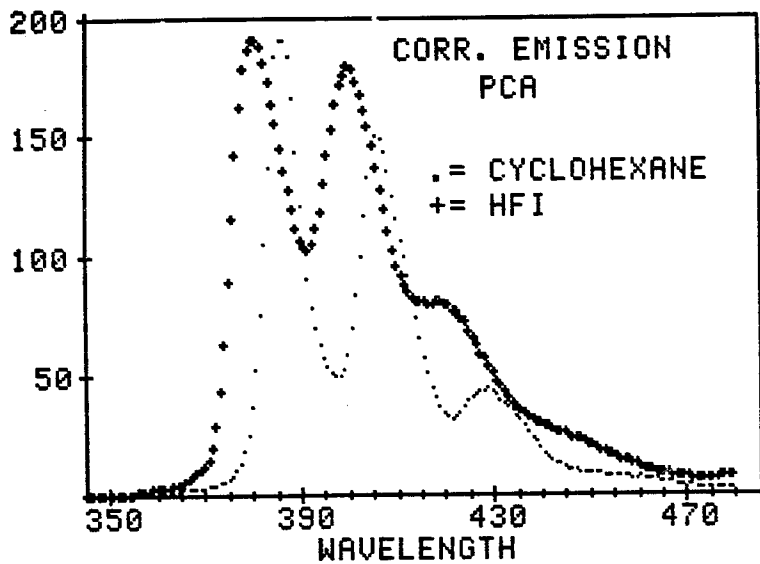


FIGURE 25

Emission Spectrum of 1-AA in Dioxane

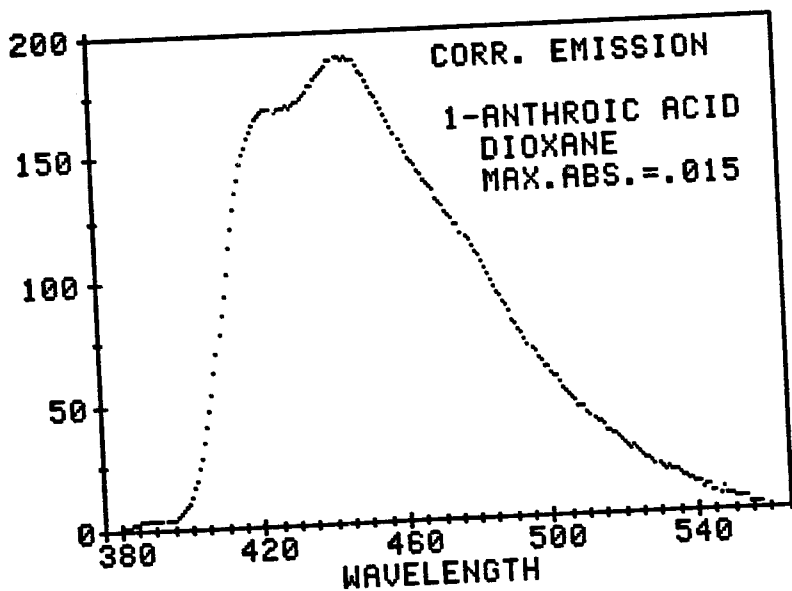


FIGURE 26

Emission Spectrum of 1-AA in Ethanol

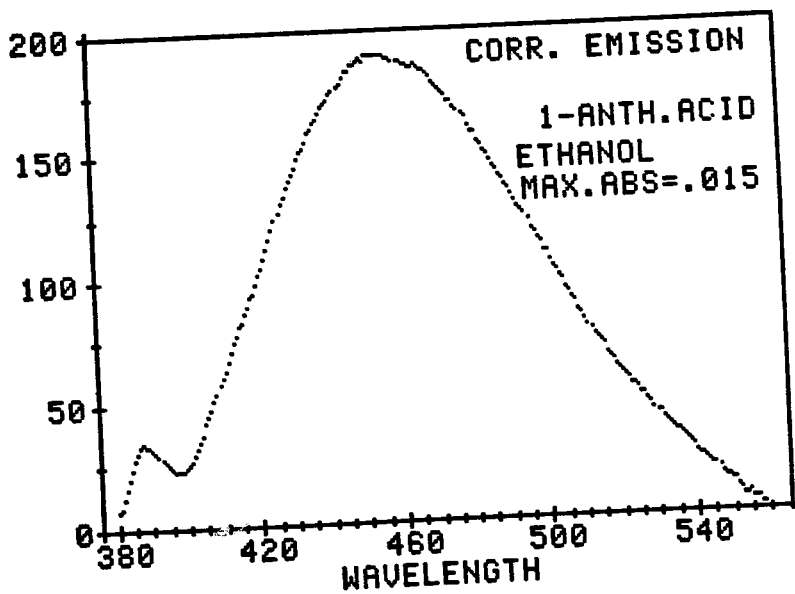


FIGURE 27

Emission Spectrum of 1-AA in Ethyl Acetate

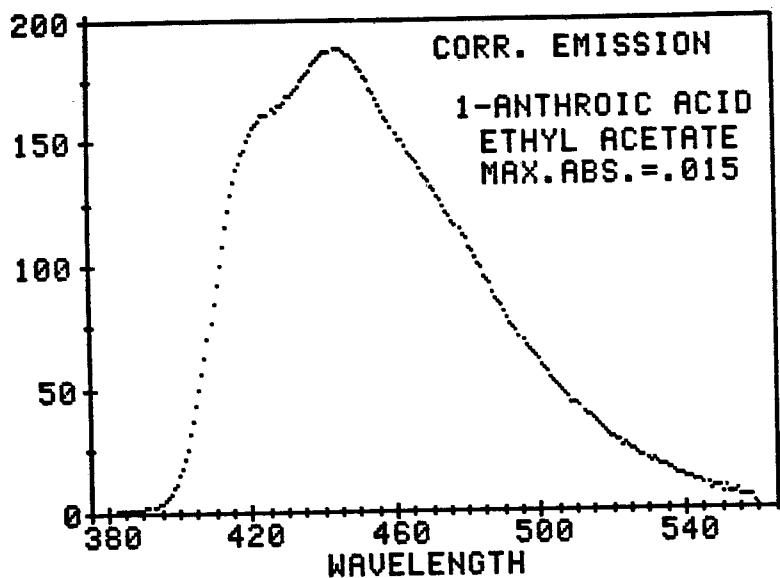


FIGURE 28

Emission Spectrum of 1-AA in Trifluoroethanol

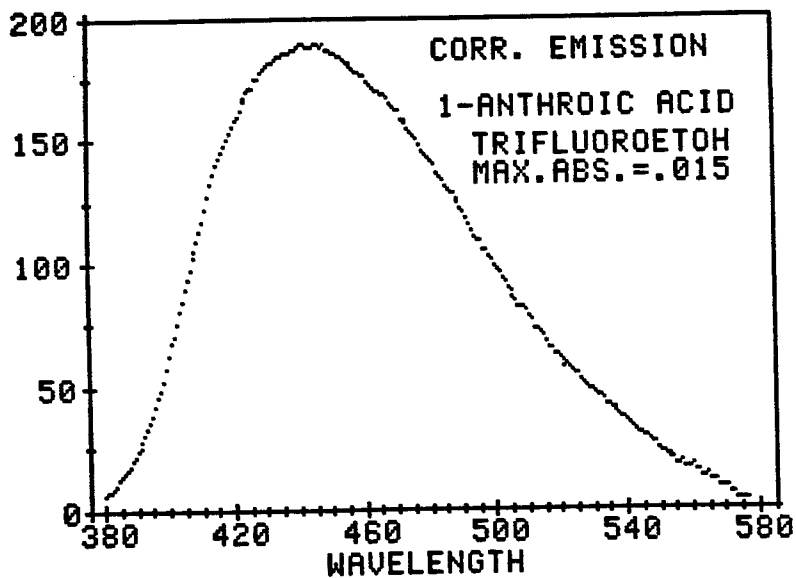
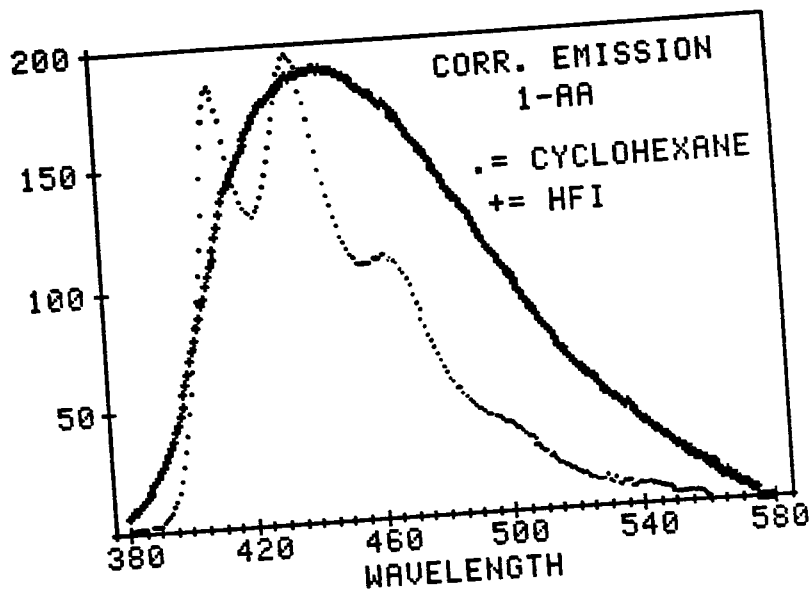


FIGURE 29

Emission Spectra of 1-AA in Hexafluoroisopropanol and Cyclohexane



Figures 30-34. The spectrum in cyclohexane is highly structured, but in the other solvents it is much more diffuse. As was observed for 1-AA, the spectrum in each solvent was red-shifted relative to that observed in cyclohexane. The solvent dependent fluorescence is evident in Figure 34. It should be noted that the emission spectrum in hexafluoroisopropanol may actually be that of PAA complexed with hexafluoroisopropanol. The spectrum has a strange shape; the fluorescence intensity increases more slowly with wavelength than is usually observed on the high energy side of the peak and it is also more red-shifted than would be expected, even in hexafluoroisopropanol. Additional solvent studies were performed to investigate the effect of hydrogen bonding in hexafluoroisopropanol on the spectral properties of PAA in both the ground and excited states, and the results are presented in Figures 35 and 36, respectively. It should be noted that after a small amount (10 μ L) of hexafluoroisopropanol was added to PAA in 10 mL of cyclohexane the spectrum changed considerably in both figures. The significance of this will be explained in the discussion.

A comparison of the spectral shifts relative to cyclohexane for each of the three molecules studied is made in Table 4. The spectral shifts for PCA were calculated using the 0-0 bands of fluorescence, because the 0-0 band was easily distinguished in all solvents. The location of the 0-0 band of 1-AA and PAA could not be determined in all solvents; therefore, the mean wavenumber was used to calculate the spectral shifts.

The spectra of PCA in ten solvents were analyzed according to the Lippert equation (equation 5) (1)

$$\bar{\nu}_a - \bar{\nu}_f = (2/hc) \left\{ \left[\frac{(\epsilon - 1)}{(2\epsilon + 1)} \right] - \left[\frac{(n^2 - 1)}{(2n^2 + 1)} \right] \right\} \left[\frac{(\mu^* - \mu)^2}{a^3} \right] + \text{constant} \quad (5)$$

in order to determine the type of solvent effects present. The quantity $\left\{ \left[\frac{(\epsilon - 1)}{(2\epsilon + 1)} \right] - \left[\frac{(n^2 - 1)}{(2n^2 + 1)} \right] \right\}$, where n and ϵ are the refractive index and the dielectric constant, respectively, of the solvent, is called the orientation polarizability (Δf). A plot of Δf

FIGURE 30

Emission Spectrum of PAA in Dioxane

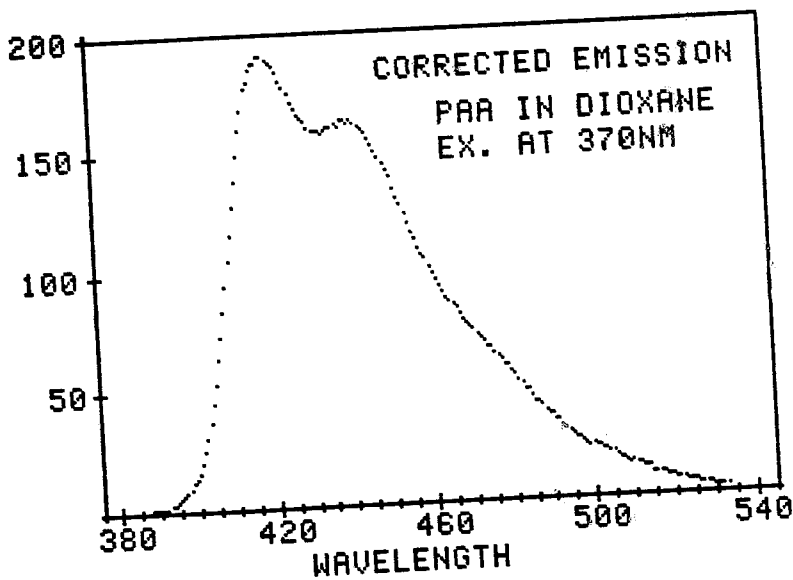


FIGURE 31

Emission Spectrum of PAA in Ethanol

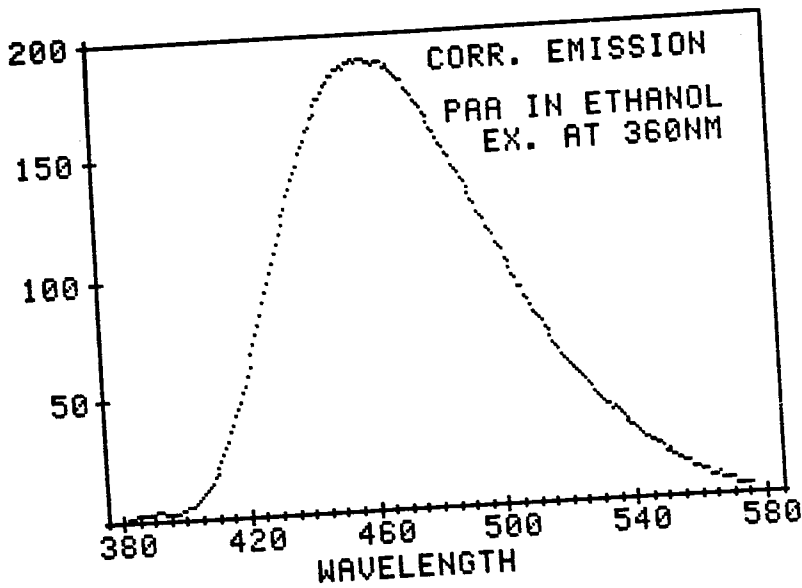


FIGURE 32

Emission Spectrum of PAA in Ethyl Acetate

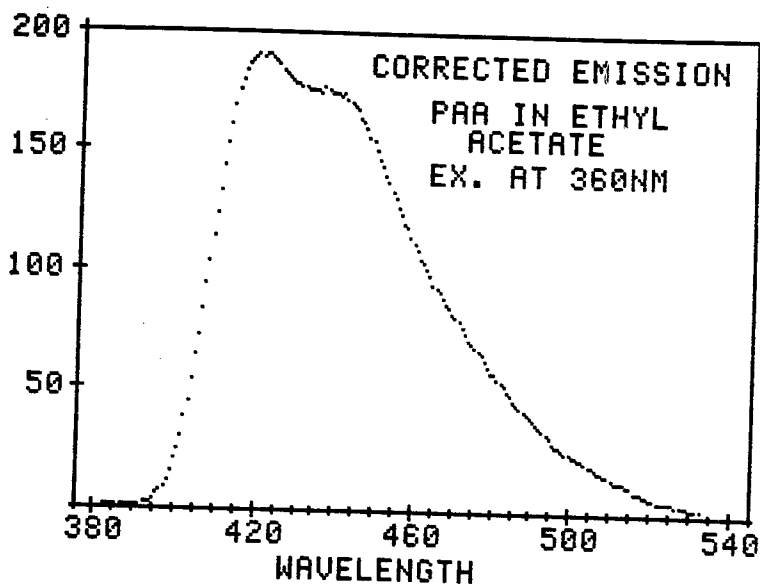


FIGURE 33

Emission Spectrum of PAA in Trifluoroethanol

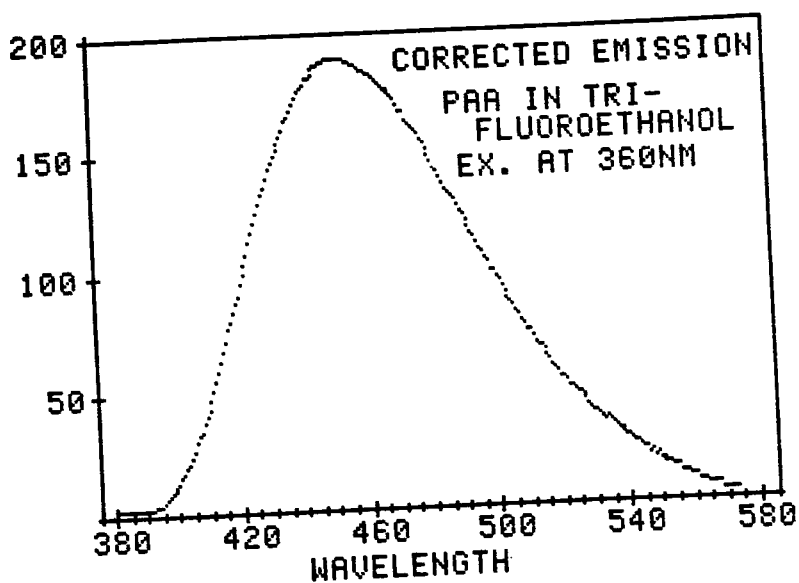


FIGURE 34

Emission Spectra of PAA in Hexafluoroisopropanol and Cyclohexane

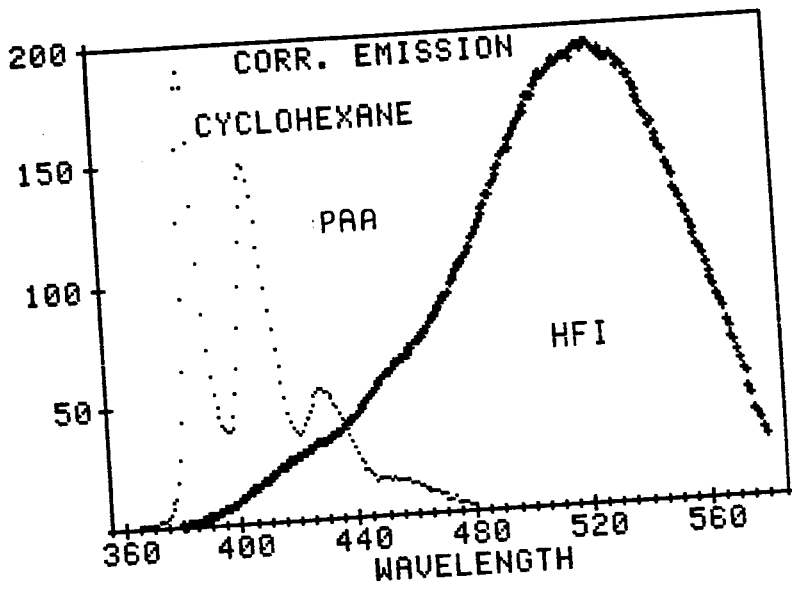


FIGURE 35

**PAA Absorption in Cyclohexane Before and After
the Addition of Hexafluoroisopropanol**

ABSORPTION SPECTRUM OF PAA
IN CYCLOHEXANE

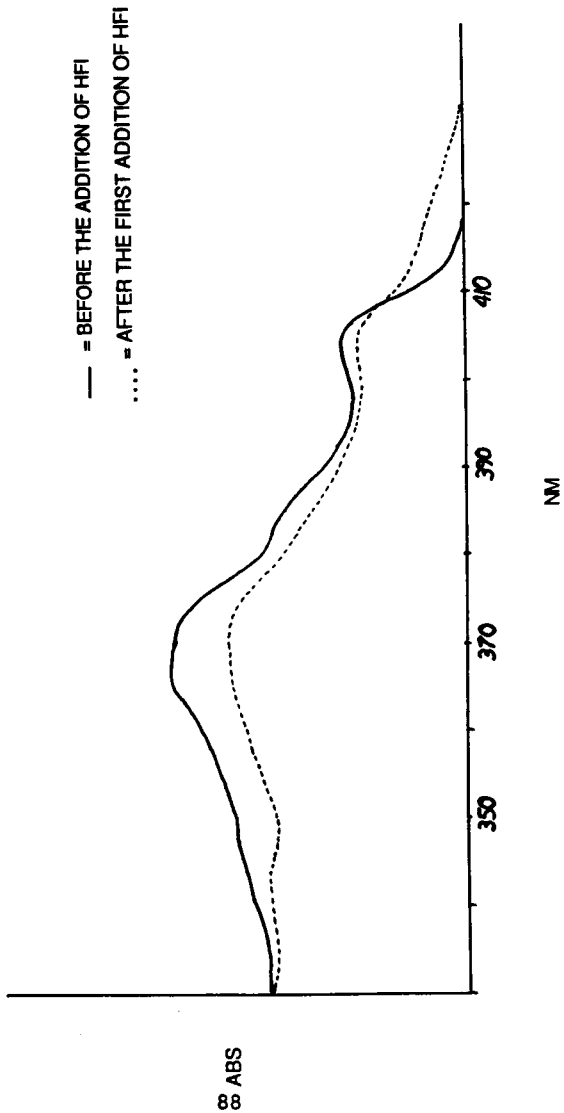


FIGURE 36

**PAA Emission in Cyclohexane Before and After
the Addition of Hexafluoroisopropanol**

FLUORESCENCE EMISSION SPECTRUM OF PAA IN CYCLOHEXANE

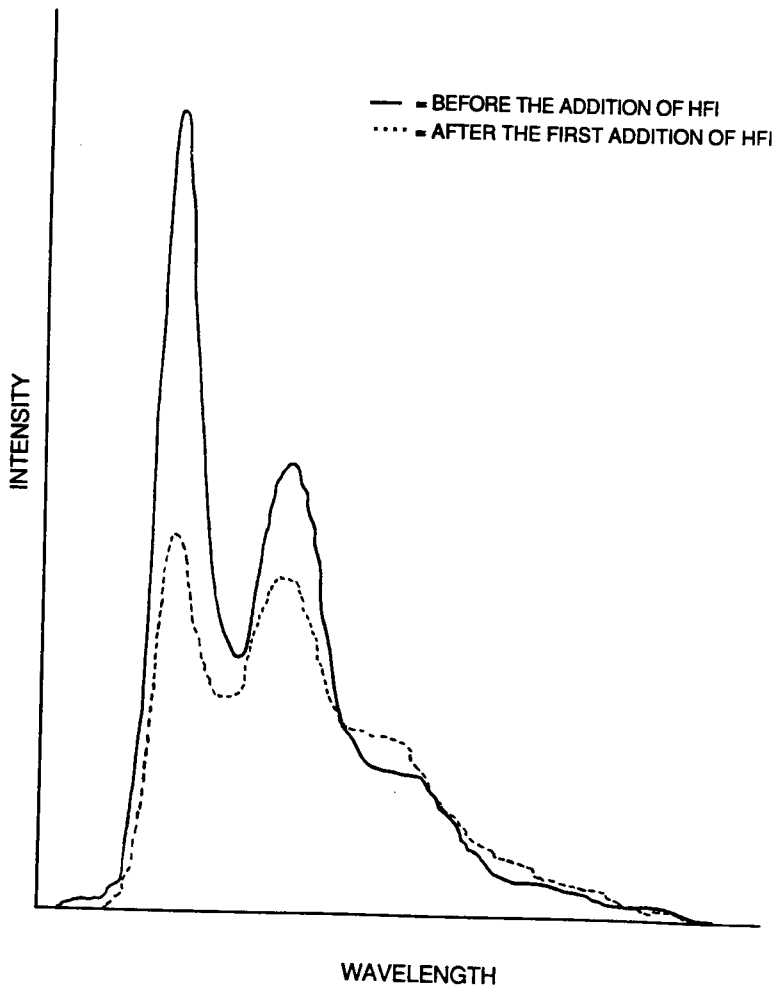


TABLE 4

Spectral Shifts^a Relative to Cyclohexane

SOLVENT	PCA^b	PAA^c	1-AA^c
Cyclohexane	0	0	0
Dioxane	-100	-1900	-600
Ethyl Acetate	0	-2000	-600
Ethanol	-100	-3400	-1200
Trifluoroethanol	+400	-3200	-1000
Hexafluoroisopropanol	+400	-5300	-1100

^aSpectral shift reported in wavenumbers

^bSpectral shift calculated using the 0-0 bands of fluorescence

^cSpectral shift calculated using the mean frequency of fluorescence

versus $(\bar{\nu}_a - \bar{\nu}_f)$, where $\bar{\nu}_a$ and $\bar{\nu}_f$ are the wavenumbers of the 0-0 absorption and fluorescence band, respectively, indicates the type of solvent effects present (1). A linear plot indicates that only general solvent effects are present. These effects are due to the motion of electrons in the solvent molecules and the dipole moment of the solvent molecules, and are expected for fluorophores in all solvents. A nonlinear plot indicates that specific solvent effects as well as general solvent effects are present. Specific solvent effects include hydrogen bonding and complexation - chemical interactions between the fluorophore and the solvent.

The Lippert plot for PCA is shown in Figure 37. It is very difficult to draw any conclusive evidence about the solvent effects on PCA from this plot because the Stokes' shifts are so small. The Stokes shifts for 9-methylanthracene and 1-aminonaphthalene are greater than 4000cm^{-1} for a number of solvents (1), making it relatively simple to determine whether the plots are linear or nonlinear. For PCA the largest Stokes shift is less than 550cm^{-1} , approximately one sixth of the smallest reported shift for 9-methylanthracene or 1-aminonaphthalene; therefore, any experimental error incurred in determining the Stokes shifts would produce a greater relative error for PCA than the other two molecules. Taking the error into consideration it can not be determined whether the Lippert plot for PCA is linear or nonlinear.

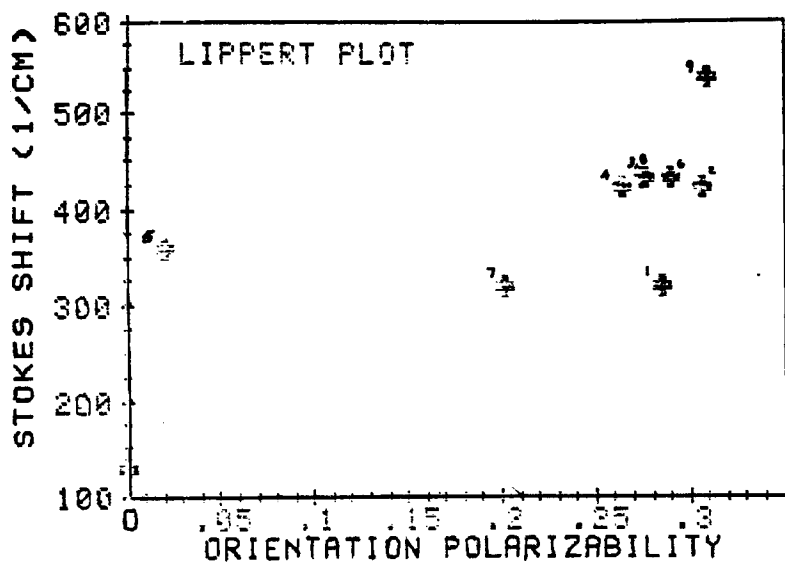
A second method used to analyze solvent effects on the fluorescence of PCA was a parameterization method based on linear solvation energy relationships. A correlation was made between fluorescent energy and the Kamlet, Abboud, and Taft parameters of equation 6 (13).

$$\bar{\nu}_f = (\bar{\nu}_f)_0 + s\pi^* + a\alpha + b\beta \quad (6)$$

The 0-0 fluorescence band in the solution under study is $\bar{\nu}_f$, $(\bar{\nu}_f)_0$ is the 0-0 fluorescence band in a reference solvent (cyclohexane), π^* expresses the polarity of

FIGURE 37

Lippert Plot



the solvent, α is a measure of the hydrogen bond donor ability of the solvent, and β is a measure of the hydrogen bond acceptor ability of the solvent. The s , a , and b coefficients are a measure of the relative susceptibilities of a molecule to the corresponding solvent properties. Reasonable coefficients were not obtained for PCA by this method because the Stokes shifts were too small to obtain a good fit of the equation.

This method was also used to determine s , a , and b values for 1-AA and PAA but a variation was made in equation 6. The fluorescence spectra of these molecules were much more diffuse than those of PCA and the 0-0 band could not be determined in all solvents; therefore, the mean wavenumber of fluorescence was substituted for the wavenumber of the 0-0 band as a measure of the fluorescence energy. Two equations with two unknowns were solved simultaneously, and values for the two unknowns were obtained.

The equations used and the values of s , a , and b obtained for 1-AA are listed in Table 6. The linear solvation energy equations for dioxane (A) and ethyl acetate (B) were solved simultaneously to obtain values for s and a . Likewise, the equations for hexafluoroisopropanol (C) and trifluoroethanol (D) were solved to obtain values for s and b .

The equations used and the values of s and a obtained for PAA are listed in Table 8. No value was determined for b ; the determination of b would have required the use of the mean wavenumber of fluorescence of PAA in hexafluoroisopropanol, and a valid value could not be obtained due to the fact that emission was proposed to occur from a hydrogen-bonded complex.

Simple molecular orbital calculations for PCA, 1-AA and PAA were performed using the Pascal program Hückel Molecular Orbitals (14). The results are listed in Table 9.

TABLE 5

Data for Determination of s, a, and b for 1-AA from the Kamlet, Abboud, Taft Parameterization Method

Solvent	π^*	α	β	$\bar{v}_m, \text{cm}^{-1}$	$\bar{v} - (\bar{v}_f)_0, \text{cm}^{-1}$
Cyclohexane	0.0	0.0	0.0	22590 ^a	-
Dioxane	0.55	0.37	0.0	22010	-580
Ethyl Acetate	0.55	0.45	0.0	21970	-620
HFI	0.65	0.01	.96	21500	-1090
TFE	0.73	0.01	.51	21600	-990

^a(v_f)₀

TABLE 6

Calculation of s, a, and b for 1-AA

Equation ^a	s	a	b
(A) $-580 = s(.55) + a(.37)$			
(B) $-620 = s(.55) + a(.45)$	-720	-500	-
(C) $-1090 = s(.65) + b(1.96)$			
(D) $-990 = s(.73) + b(1.51)$	-660	-	-340

^afrom eqn. 6, $\bar{v} - (\bar{v}_f)_0 = s\pi^* + a\alpha + b\beta$

TABLE 7

Data for Determination of s and a for PAA from the Kamlet, Abboud, Taft Parameterization Method

Solvent	π^*	α	β	ν_m, cm^{-1}	$\bar{\nu} - (\bar{\nu}_f)_0, \text{cm}^{-1}$
Cyclohexane	0.0	0.0	0.0	24600 ^a	-
Dioxane	0.55	0.37	0.0	22700	-1900
Ethyl Acetate	0.55	0.45	0.0	22600	-2000

^a(ν_f)₀

TABLE 8

Calculation of s and a for PAA

Equation ^a	s	a	b
(A) $-1900 = s(.55) + a(.37)$			
(B) $-2000 = s(.55) + a(.45)$	-1300	-2600	-

^afrom eqn. 6, $\bar{\nu} - (\bar{\nu}_f)_0 = s\pi^* + a\alpha + b\beta$

TABLE 9

Results of Molecular Orbital Calculations

Compound	% increase in π b.o. at C_1^a in S_1	% increase in ρ^b at O_1^c in S_1	% increase in ρ at O_2^d in S_1
1-AA	13.8	2.14	.605
PCA	13.4	1.50	.637
PAA	10.2	1.22	.560

^a C_1 is the carbonyl carbon

^b ρ = charge density

^c O_1 is the carbonyl oxygen

^d O_2 is the hydroxyl oxygen

DISCUSSION

In order to make a good comparison of the absorption spectra of the three compounds studied, the concentration of each compound in the various solvents should have been kept constant. Concentrations were not kept constant; therefore, it is only possible to make a generalization about the absorption spectra. At the concentrations used, the absorption of 1-AA was solvent dependent - the shape and the location of the spectrum varied in different solvents, while the absorption of both PCA and PAA exhibited a solvent dependence only in highly protic solvents. The results of both the pK_a determinations and the solvent studies indicate that the geometry of PCA in the S_0 and S_1 states is similar. The experimentally determined pK_a and pK_a^* of PCA are within one pH unit ($\Delta pK_a < 1$) of each other (Table 1). In comparison, ΔpK_a for 9-anthric acid is reported to be much larger - values of 3.2 and 3.5 have been obtained (4). The large ΔpK_a is indicative of a significant shift of electron density to the carboxyl group upon excitation, making S_1 a much stronger base than S_0 . The shift of electron density results in the formation of a CT state. It has been proposed that the formation of this CT state in the excited state is made possible by the rotation of the carboxyl group to a coplanar configuration with the ring (4). As a result of the rotation, the ground and excited states of 9-anthric acid must have significantly different geometries.

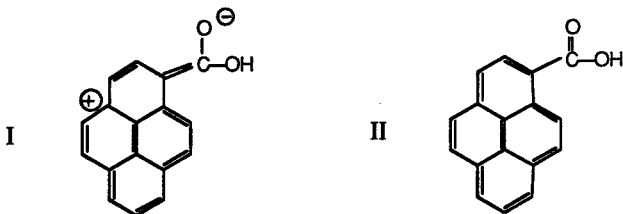
The small ΔpK_a^* for PCA indicates that there is only a small shift of electron density to the carboxyl group upon excitation. Because the S_1 state is only slightly less acidic than the S_0 state, the geometry of S_1 must be similar to that of S_0 ; therefore, it is

unlikely that the carboxyl group undergoes rotation to a more coplanar position with the ring upon excitation. It should be noted that the pK_a^* values did not show a buffer dependence. This implies that an excited state equilibrium was attained, and the value of the pK_a^* obtained was a true measure of the acidity of the excited state.

The pK_a^* 's calculated from the Förster cycle are greater than the experimentally determined values. In determining the validity of the calculated pK_a^* 's, it must be taken into consideration that the accuracy of Förster cycle calculations is dependent upon certain assumptions and if the assumptions do not hold true the pK_a^* can not be considered chemically significant (6). It must also be remembered that the pK_a^* is dependent upon the value determined for the pK_a . Considering the uncertainties present in Förster cycle calculations and the fact that the experimentally determined pK_a^* was obtained in an equilibrium condition, the validity of the calculated pK_a^* 's is more questionable than that of the experimentally determined pK_a^* 's.

The results of the solvent studies on the fluorescence of PCA support the conclusion drawn from the pK_a analysis, namely that the geometry of the S_0 and S_1 states of PCA are similar. PCA has a solvent independent fluorescence (Figures 20-24). The small spectral shifts and the retention of structure in solvents of varying polarity, particularly solvents which are highly protic, indicates that fluorescence probably does not occur from a CT state; therefore, the carboxyl group probably does not undergo rotation to a coplanar position with the ring, because this would allow for charge transfer to the vacant π orbitals of the carboxyl group.

Although quantitative analysis by the Kamlet, Abboud, and Taft parameterization method did not produce any numerical results pertaining to the molecular properties of PCA, the lack of these values supports the assumption that PCA must not undergo a significant change of geometry upon excitation. If a large shift of electron density to the carboxyl group occurred upon excitation then structure I would have to be considered



as an excited state resonance form. Structure I would be expected to exhibit more solvent dependence than structure II in which there is no charge transfer because I is more susceptible to hydrogen bond formation in polar protic solvents. The fact that no values could be determined for PCA's susceptibility to hydrogen bond formation or polarization as a result of its solvent independent fluorescence even in polar protic solvents indicates that fluorescence occurs primarily from II rather than I.

Values of 3.7 and 6.9 for the pK_a and pK_a^* , respectively, of 1-AA in aqueous solution have been reported (6). The ΔpK_a can be calculated from these values - $\Delta pK_a = 3.2$. The large ΔpK_a indicates that there must be a significant shift of electron density to the carboxyl group upon excitation.

The fluorescence spectra in Figures 25-29 indicate that the fluorescence of 1-AA is solvent dependent. There are significant spectral shifts (Table 4) in solvents of varying polarity and there is a loss of structure in polar solvents. This is in agreement with previous studies (16).

1-AA was also analyzed according to the Kamlet, Abboud, and Taft parameterization method; the data and results are listed in Tables 5 and 6. The fluorescence of 1-AA is known to be solvent dependent; therefore, it was expected that values would be obtained for s , a , and b . Values were obtained and as expected they indicate that 1-AA is susceptible to polarization and hydrogen bond formation. The

obtainment of values of s , a , and b for 1-AA indicates that this method can be used to assess molecular properties, so the fact that no values were obtained for PCA is not the result of an unrealistic method of analysis.

It is difficult to report an accurate value for the ΔpK_a of PAA because the values obtained for the pK_a^* (Table 1) indicate a buffer dependence, which implies that an excited state equilibrium was not reached; therefore, the values obtained for the pK_a^* can not be considered a true measure of the acidity of the excited state. There are two factors which determine whether equilibrium will be established in the excited state. One factor is the lifetime of the excited state, and the other is the rate of proton transfer in the excited state. If the excited state lifetime is very short or if the rate of proton transfer is slow, an excited state equilibrium may not be reached. Because excited state lifetime measurements were not made, it can not be said which factor is more significant in the case of PAA. There is also another reason why the ΔpK_a is subject to question. Although the pK_a of PAA was determined, the validity of the value is questionable. An isosbestic point was not observed in the absorption spectra of PAA as a function of pH; therefore, the acid-base reaction may have been complicated by other phenomena. If that is the case, then other factors must be taken into consideration in the calculation of the pK_a , and the simple method of analysis which was used (equation 1) does not provide accurate results.

Large values for the ΔpK_a of PAA were obtained from the Förster cycle calculations. As was stated previously, these values are sometimes questionable, but they do indicate a much larger ΔpK_a for PAA than for PCA; this is in agreement with the experimental results. If results were obtained at high enough buffer concentrations to ensure that an excited state equilibrium was reached, the values obtained for the pK_a^* would be greater than the values that were obtained. This would indicate that $\Delta pK_a > 2$. Förster cycle calculations for PAA which were based on fluorescence data indicate that $\Delta pK_a \geq 3.8$ (Table 3), depending on the method chosen. Values of ΔpK_a for PCA

obtained from the Förster cycle calculations were larger than the ΔpK_a which was determined experimentally; therefore, it is likely that experimentally determined ΔpK_a is in the range $2 < \Delta pK_a < 3.8$.

The large ΔpK_a indicates that the S_1 state of PAA is considerably more basic than the S_0 state. This implies that there must be a significant shift of electron density to the carboxyl group upon excitation. In order for this shift of electron density to occur, the carboxyl group probably undergoes rotation to a more coplanar position with the ring.

The solvent dependent fluorescence of PAA implies that fluorescence occurs from a CT state. The large spectral shifts (Table 4) and the diffuseness of the spectra in polar solvents are indicative of fluorescence from a CT state. The formation of a CT state indicates that charge was transferred to the carboxyl group; therefore, the results are consistent with the results obtained in the pK_a analysis.

Analysis of PAA by the Kamlet, Abboud and Taft parameterization method indicated that PAA is more susceptible to polarization and hydrogen bond donation than 1-AA is. No value was determined for b , the susceptibility to hydrogen bond acceptance, because it was determined that PAA undergoes complexation in hexafluoroisopropanol; therefore, the value obtained for the spectral shift in hexafluoroisopropanol was not valid to use in the calculation of b .

The conclusion that PAA undergoes complexation with hexafluoroisopropanol was based on the spectra in Figures 35 and 36, which represent the results obtained from the studies performed to investigate the effects of hydrogen bonding in hexafluoroisopropanol on the spectral properties of PAA. Both the absorption and fluorescence spectra of PAA in cyclohexane change with the addition of small amounts of hexafluoroisopropanol. It has been suggested that the perturbation of the fluorescence spectra of some aromatic compounds in nonpolar solvents by the addition of small amounts of a protic solvent is due to the formation of a hydrogen-bonded complex (15). The amount of hexafluoroisopropanol added to the

solutions of PAA in cyclohexane was not large enough to alter the dielectric properties of the cyclohexane; therefore, the change in each spectrum indicates that PAA must form a hydrogen-bonded complex with hexafluoroisopropanol in both the ground and excited states.

In conclusion it can be stated that the ground states of the pyrene carboxylic acids exhibit similar properties, but the excited states do not. The addition of the CH=CH group as part of the substituent group on PAA may allow for more extensive conjugation of the substituent with the ring and freer rotation of the substituent in the excited state. This would result in a greater transfer of charge to the vacant π orbitals of the carboxyl group and would account for the differences observed in the S_1 states of the acids.

REFERENCES

- (1) J. R. Lakowicz *Principles of Fluorescence Spectroscopy*; Plenum: New York, 1983.
- (2) D. A. Skoog *Principals of Instrumental Analysis III Edition*; CBS: USA, 1985.
- (3) T. C. Werner In *Modern Fluorescence Spectroscopy 2*; E. L. Wehry, Ed.; Plenum: New York, 1976, 277-316.
- (4) T. C. Werner and D. M. Hercules *J. Phys. Chem.*, **1969**, *73*, 2005-2011.
- (5) T. C. Werner and D. M. Hercules *J. Phys. Chem.*, **1970**, *74*, 1030-1037.
- (6) S. G. Schulman In *Modern Fluorescence Spectroscopy 2*; E. L. Wehry, Ed.; Plenum: New York 1976, 239-274.
- (7) T. C. Werner *User's Manual for the Apple/MPF-2A Interface*, 1986.
- (8) J. M. Oton and A. U. Acuna *J. of Photochemistry*, **1980**, *14*, 341-343.
- (9) H. H. Jaffe and M. Orchin *Theory and Applications of Ultraviolet Spectroscopy*; John Wiley and Sons: New York, 1962, 562-563.
- (10) Vander Donkt et al. *Trans. Far. Soc.*, **1969**, *65*, 3258.
- (11) Escabi-Perez and Fendler *J. of Amer. Chem. Soc.*, **1978**, *100*, 2234.
- (12) T. C. Werner and D. B. Lyon *J. of Photochemistry*, **1982**, *18*, 355-364.
- (13) T. C. Werner and D. B. Lyon *J. Phys. Chem.*, **1982**, *86*, 933-939.
- (14) John J. Farrel *Hückel Molecular Orbitals*, 1985.
- (15) Takashi Tamaki *Bull. Chem. Soc. Jpn.*, **1982**, *55*, 1761-1767.
- (16) T. C. Werner, Thomas Matthews, and Babs Soller *J. Phys. Chem.*, **1976**, *80*, 533-541.